Synthesis of Reusable functional magnetic chitosan adsorbent beads for the removal of Cr (VI) from water

By

Sana Shahid

School of Chemical and Materials Engineering

National University of Sciences and Technology

2021

Synthesis of Reusable functional magnetic chitosan adsorbent beads for the removal of Cr (VI) from water

Name: Sana Shahid

Reg No.: 00000276812

This thesis is submitted as partial fulfilment of the requirements for the Degree of

MS in Materials & Surface Engineering

Supervisor: Prof. Dr. Nasir M. Ahmed

School of Chemical and Materials Engineering (SCME)

National University of Sciences and Technology (NUST)

H-12 Islamabad, Pakistan

December, 2021

Dedication

I would like to devote my

Thesis

To my beloved Family and

Supervisor.

Acknowledgements

All praises to Almighty Allah, whose greatness can never be explained by the words. His blessings can't be calculated. I am thankful to my creator for providing me chance to gain knowledge and giving me enough strength to carry out this research. In my research journey I found a mentor, a role model, an inspiration and a firm support in the form of my supervisor Prof. Dr. Nasir M. Ahmed. He was always there to support and encourage me. His guidance and advices during the research phase were priceless. Without him this thesis would have been impossible. It was an honor and pleasure working under sir's supervision. I am extremely grateful to my GEC members for their support and assistance, as they helped me in characterization of my sample. My words are insufficient to pay gratitude to my parents and sibling their love, prayers, affection and encouragement are asset of my life. The moral support of my friends, Rida, Majida, Momina, Shehla were always there for me. Without them this journey would have been much difficult.

Sana Shahid

Abstract

Industries along with industrial sites across the world are a major contributor of heavy metal pollution in water, among which Chromium possess the most toxic effects. To overcome this problem a productive method is needed for the removal of Chromium from water. In this regard, Beads based on chitosan, a non-toxic, biocompatible and biodegradable polymer, have showed great potential in numerous applications, including the removal of heavy metals from water. In this study Nano scale Iron Oxide particles produced by Sol Gel method were embedded in chitosan by using chemical co-precipitation method. The performance of Iron Oxide embedded chitosan beads (IECB) has been studied in a batch system, for chromium (VI) adsorption from industrial water specially. Concentration of chromium in solution was determined via UV Vis spectrophotometry on the basis of yellow color of chromate ions. Physiochemical properties of IECB were characterized through XRD, SEM, FTIR, VSM, contact angle and BET. Multiple factors influencing the adsorption attitude of IECB such as pH, temperature, initial concentration and interaction time of chromium ions were measured and 23.9 mg/g was the maximum adsorption capacity obtained at pH=4, 70◦ C in 6 hrs. In this study, the Langmuir isotherm model (R^2 > 0.991) and pseudo second order kinetics (R^2 > 0.984) best fitted the experimental data. Moreover, thermodynamic parameters explain the Cr (VI) removal rate of Iron Oxide embedded chitosan (IEC) beads, which was maintained as high as 93.4% and 87% on the 4th and 5th runs respectively and at the end beads were successfully regenerated.

Table of contents

List of figures

List of tables

Abbreviations

IECB	Iron Oxide embedded chitosan beads
CrO_4^{2-}	Chromate
$Cr_2O_7^{2-}$	Dichromate
Ce	Equilibrium conc. (mg/l)
Co	Initial conc. (mg/l)
Kl	Langmuir constant
Kf	Fraundlich constant
n	Fraundlich exponent
q_e	Equilibrium adsorption (mg/g)
Q_t	Adsorbed amount at time "t" (mg/g)
$k1$	Pseudo-first order rate constant (l/min)
e	Exponential function
Fe_2O_3	Ferric oxide
OH	hydroxyl group
NaOH	Sodium Hydroxide
$FeCl_3.6H_2O$	Iron (III) Chlorid Hexahydrate
$(C_2H_2OH)_2$	Ethylene Glycol
$(FeCl_2.4H_2O)$	Iron (II) Chlorid Tetrahydrate
$(C_6H_{11}NO_4)$ n	Chitosan

Chapter 1-Introduction

1.1 Environmental pollution

Disadvantageous variation of our surroundings is the environmental pollution due to entirely or mainly as a result of man's activities, through various unlimited consequences of the alteration in the energy levels, features of fumes, and chemical and other regulations and plenty of micro-organisms. Environmental pollution is a major global problem and especially it is common to all countries, which attracts the curiosity of specially human beings for its drastic everlasting outcomes.

Environmental quality has been declined because of pollution and it is confirmed by the deprivation of flora, biological distinctiveness, and unrestricted amounts of injurious alchemicals in the surrounding environment along within food chains specially, and increasingly instable experiments of environmental mishaps and ultimatum to life saving mechanisms particularly.

By different type of people it (Pollution) is perceived from various angles in terms of thinking which is generally accepted to be the consequences of urban industrial and chemical insurgency and fast ill treatment of naturally occurring resources, enhanced rate of interchange of matter along with energy, and all time expanding industrial rubbish, cities discharge, and consumer products [1].

Environmental pollution can also be addressed as an establishment by mankind, into the surrounding, of components accountable to principle source disturbance with permissible utilization of the circumstances [2]. In a simplest way environmental pollution can be defined as non-equilibrium situation from equilibrium situation in any system [3]. This concept might be practiced to all types of environmental pollutions ranging from somatic to economic, political, and other environments. Since past few years, numerous sources of environmental pollution has been discovered that has been adapt the formation of water, air, fire and soil of the environment.

The materials that are responsible for the contamination are called pollutants. A pollutant material can be split up into any harmful alchemical (poisonous metals/non-metals, radionuclidas, organo phosphorus chemical compounds, gaseous materials) or geo-chemical materials (dirty, remainings), biological compounds or materials, or earthly substances (heat, sound waves) that is dispatched deliberately or accidentally by mankind into the surrounding together with real or potential unfavourable, dangerous, pleasant, or unsuitable impact.

Such unacceptable consequences might be direct (affecting mankind) or indirect, being moderate through resource components or weather variation. On the basis of type of pollutants along with the successive pollution of environmental organisms, the environmental pollution can be classified as following:

1. Water contamination
2. Air contamination
3. Noise contamination
4. Land contamination
5. Thermal contamination
6. Radioactive contamination

Among these types of contaminations, Water contamination is the main type which is threatening our environment, human activities and all living organisms [1].

1.2 Water pollution

Planet earth is primarily composed of water. Marine environment usually enfold more than 2/3 of the Earth's surface. And Earth’s life depends on water to survive. Where, water pollution is an actual warning to our survival on earth. According to world’s most influential people this problem is not only threatening for human’s but also for plants and animals along with other living organisms [4].

Commonly as a consequence of human acts, water surfaces become polluted which causes water pollution. Lakes, seas, rivers, oceans, aquifers and ponds are few examples of water bodies. Due to the introduction of contamination in to the natural environment, water pollution related problems originated. Water contamination is the foremost global cause of deaths and diseases, e.g. because of water-originated diseases. [5] [6]

Water contamination can be categorized as pollution of surface and ground water. Seawater contamination and nutrient contamination are basically subgroups of water contaminations. Point origin or non-pointed origin are two famous origins of water pollution. Its origin have many distinguishable source of the pollution i.e. a storm sewer or a waste water therapy foundry. Non-point origins are particularly more dispersed, such as acidic rainfall etc. [7]

Industrial waste is the major cause of the water pollution. Trash produced due to industrial tasks composed of any useless and harmful material and it is produced due to some industrial processes which consists of manufacturing activities in business unit, industries tasks, mills waste, and extracting operational affairs.

Variety of waste like from corporation comprises of dust material and shingles, brick-wall and hard, waste metal elements, oil particles, alchemical materials, chemical compounds, even food stuffs/fruits materials specially from cafeteria [8]. Mills waste material also includes heavy metal ions such as mercurey (Hg), cadmim (Cd), arsenice (As), chromim (Cr), thallium (Tl), lead (Pb) and nickel (Ni) etc. which possesses high solubility in water. [8]

So problems regarding pollution of water, due to presence of heavy metal ion's waste is discussed briefly in this chapter.

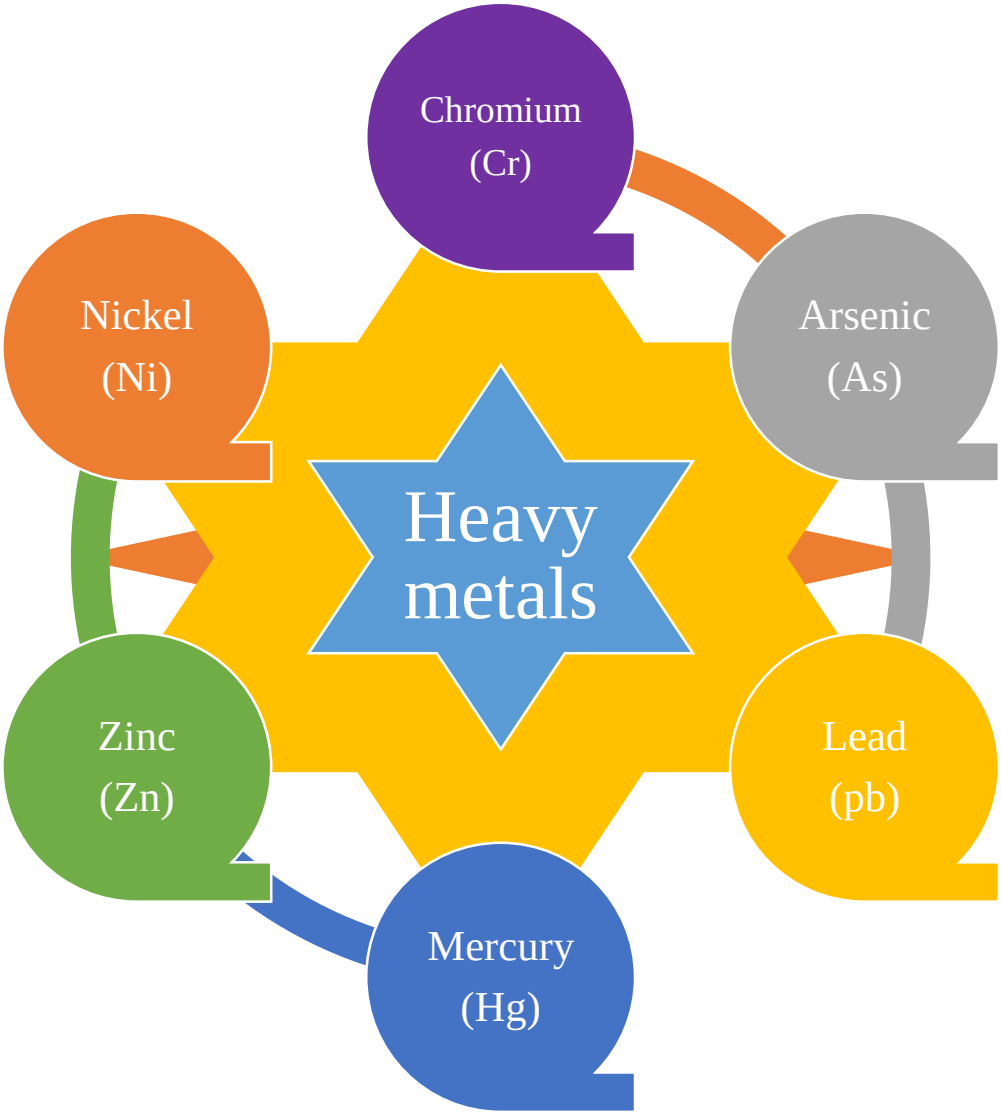

Figure 1: Various heavy metals present in water

1.3 Heavy metals

Heavy metals are usually explained as naturally appearing elements with correlative high atomic weights, or increased atomic numbers and density that is approximately five times higher than that of water. [9] Heavy metals have received an overriding attention among all other pollutants, to ecological chemists because of their poisonous nature. Heavy metals are poisonous even at very small quantities and they are generally exists in very small concentration in natural waters. [10]

Heavy metal ions such as chromim, arsenec, lead, cadmium, mercury, nickal, cobalt, zinc and seleniam are very poisonous even in minute amount. With the passage of time increasing amount of heavy metals is a process of substantial importance. Currently a many industries are pouring out their pollutants containing metals and nonmetals into clean water without any sufficient further treatment. [11]

When elements especially poisonous metallic ions are not penetrated by the body they become toxic and gradually assembled in the soft tissues. Human body can usually absorb them through particles of bread, water droplets, air and integration through the face pores while these chemicals come in contact with human beings in agriculture, medicine, manufacturing, fabrication settings or domestic activities etc.

Usually industriall disclosure is a usual way of contact for grown person. Consumption is the utmost ordinary way of contact in terms of kids. In a nutshell both genuine and people's activities are polluting the surrounding as well as its assets, because of it waste has been releasing far more than what the environment can hold. [10][12]

1.3.1 Sources of heavy metals

Both natural (volcanic discharge, sea-salt production, forest fires spread, rock crumbling and biogenic resources) and organic evolution processes (Industries toxic chemicals, agricultural waste, wastewater material, mining poisons and elements in metallurgical processes) can emanate heavy metals and arrive in various environmental sections (soile, water, aer and their intersection). [10]

1.3.2 Effects of heavy metals contamination

Hard core rock pollution is beseeming a major problem all over the world which needs to be solved as it has gained importance because of the increased use along with treatment of hard core rocks during numerous tasks to fulfill the demand of the fastly developing communities. Soil, water needs and clean air are the crucial components present in surroundings that are badly damaged by hard core rocks/ heavy metals pollution specially. [13]

Table 1: Effect of various Heavy Metals

Heavy metals	**Toxic Effects**
Chromium	Nausea, Chronic Asthma, Coughing, kidney and cardiovascular diseases.
Arsenic	Carcinogenic, Vascular disease, Skin, Kidney, Lungs disorder.
Lead	Circulatory system, Nervous system, damage the fetal brain.
Mercury	Disease of Kidney, Nervous system, Circulatory system.
Cadmium	Renal Disorder, Carcinogenic, Kidney disorder.
Zinc	Increased thirst, Depression, Lethargy.
Nickel	Diarrhea, Headache, Vomiting.

All of these heavy metals are really harmful for us. But out of these heavy core metal rocks, Chromim is one of the dominant element that creates maximum harmful effects not only on aquatic life but on human health as well. So it needs to be removed from our drinking water especially, at any cost.

1.4 Effect of Chromium

In the Earth's crust Chromium is the 21st utmost ample element along with average concentration of about 100ppm. It doesn't exist in free form usually. Because of the erosion of chromium containing rocks, chromium compounds have been founded in the environment and by volcanic eruption these compounds can be rearranged. In environmental media normal background concentration of chromium is as following:

1. In freshwater < 8-10 µg/L
2. In seawater < 0.7-1 µg/L
3. In atmosphere < 6-10 ng/m^3
4. In soil < 400-500 mg/kg
5. In vegetation < 0.6 mg/kg
6. In sediments < 80 mg/kg [14] [15]

Normally chromium found in several oxidation states, among which most common and firm forms with in chromium compounds are the hexavalant Cr (VI), the trivalant Cr (III) and Cr (0) types. The utmost toxic types of Cr (VI) are chromate (CrO_4^{2-}), dichromate ($Cr_2O_7^{2-}$) and CrO_3 particularly, as these forms presents high solubility, high oxidizing capability and especially high flexibility over the membranes in the environment and in living organisms as well.

In the appearance of oxids, hydroxids and sulphates Cr (III) possess minimum toxicity, as it maybe comparatively non-soluble or less soluble in solvent, shows less solubility, and is mostly obliged to organic compounds in aquatic environments and in soil. Furthermore, Cr (III) type tried to devise precipitates of OH with iron at normal tape water values of pH. In the presence of high percentage of O_2 and manganese, Cr (VI) can be obtained from Cr (III). Typically Cr (0) is a solid metallic form, which assembled in industry with high merging point. It is commonly utilized in the formation of good quality steel along with other durable alloys. [16] [17]

Among all oxidation states of the chromium, hexavalent form is particularly considered as the most toxic form of the chromium, whereas Chromium (III) is far less toxic relatively and causes very small/ few health issues. Chromium has very high

propensity to be caustic and due to severe immune sensitive reactions to the human body. These allergic reactions causes severe redness along with swelling of the skin. That's why one may face nose ulcers and irritability to the nose's lining, due to high inhaling levels of chromium (VI).

Other fatal human body problems include problems in tiny intestine and abdomen, harm sperm and human system related to reproduction and anemia. In the worst case of revelation of very high dosage of chromium based composites to humans, can cause serious cardiovascular, gastrointestinal, respiratory disorder, hepatic, renal problems, and neurological effects and maybe end of life. [18]

In some, in living and in non-living cases chromium compounds induces damages to DNA in several different methods and can result in the development of DNA crosslinking, chromosomal divergence, variation in repetition sister chromate swap, and specially translation of DNA. Therefore, there are numerous evidences that can prove that chromium promote carcinogenicity in humans. Moreover increased cases of intestine tumers had been detected widely in wild life and human beings specially who came in contact to chromim (VI) in fresh aquatic environment particularly. [19]

Highly focused research has been going on in order to discover the economical method for the elimination of Chromim from water used for drink due to the increasing risk of Chromim day by day on human health, animals, aquatic life and agriculture.

1.4.1 Methods to remove Cr from water

Some renowned agencies such as WHO and USEPA have specially specified an acceptable restriction of Cr (VI) in fresh marine water which is 0.05 mg/Liter in dissolved form and in case of entire Chromium (all oxidation sates of chromium) this limit is 2 mg/L. [20] In this scenario it is extremely crucial to separate Cr (VI) from waste water and drinking water or at least reduce it into Cr (iii) which is relatively less toxic to excrete into the environment.

Up till now, numerous methods have been discovered in order to minimize the injurious impact of Cr (VI) such as reversed osmosiss, ligand exchange, electrical enrichment, membrane filtration, precipitation and electrocoagulation. [21-24] These

methods had some major flaws like very huge maintaining and operating cost, low efficiency, production of harmful secondary pollutants, sludge disposal issues and particularly badly effecting human and aquatic life. [25]

Whereas adsorption process is comparatively simple to employ, cost efficient, produce very little secondary pollutants, effective method and solves the challenge of waste disposal. Adsorption is the only efficient method to eliminate all heavy metals and particularly Cr (VI) from drinking water and from industrial waste water as well. [26]

The process of transfer of organic mass from the less concentrated phase onto the outer surface of a concentrated mass is described as adsorption process. Adsorption material or adsorbent needs to have the greatest surface area along with minimum volume, in order to adsorb maximum adsorbate. Moreover, the substantial and alchemical properties of the material to be adsorbed along with the solid surface on which adsorption will occur, mainly determines the efficiency of the adsorption process. [27]

Figure 2: Methods for Removal of Chromium from Water

1.5 Adsorption Process

The bonding of ions, atoms and molecules from solid, liquid or gas to a solid surface is known as adsorption process. Collection of ions, atoms or molecules by the external as well as internal surface of the solid is also described as adsorption. In this scenario, the solid surfaces which are used to adsorb dissolved material or gases are known as adsorbents and collectively adsorbed mass is known as adsorbate.

The main difference between the adsorption and absorption is that, adsorption is a surface phenomenon and in absorption entire volume of the material take part. A general term used for both of these phenomena is known as sorption. [28]

Adsorption is considered as an outcome of surface energy, similar to surface tension. In case of bulk materials, atoms are attached with each other through different bondings like ionic, covalent, coordinate covalent, hydrogen bonding or metallic bonding. Whereas, on the surface of the adsorbent material, all atoms or molecules are not entirely attached with the other constituent atoms or atoms and that's the main reason why adsorbents can easily form bond with adsorbates. [29]

Adsorption process is commonly categorized in to:

1. Physisorption
2. Chemisorption

In nature, adsorption can either be physical or chemical. In physical adsorption (physisorption) usually weak Van der Waals forces play their role between solid adsorbent and the adsorbate molecules. At low temperature and high pressure physisorption process is more favorable. In chemical adsorption (chemisorption) normally covalent bonds formed between adsorbent and adsorbate. It is a bit slower process as compared to physisorption and it usually happens at higher temperature. [28]

1.5.1 Adsorption mechanism

The traditional process of adsorption comprises of following steps:

1. Spreading of adsorbate atoms into adsorbent surface.
2. Migration of atoms into pores of adsorbent.
3. Development of monolayer layer of material to be adsorbed on the adsorbent.

First of all due to the presence of intermolecular forces between adsorbent and adsorbate, spreading of material to be adsorbed occur on the outer adsorbent's surface. As adsorbent surface contain many pores so in second step adsorbate atoms migrated into the pores of the adsorbent surface. In the final step these adsorbate atoms will fill up the pore volume and then atoms of the adsorbate will develop the single layer of approached atoms, group of atoms and atoms to the sites of action of adsorbent. [30] [31]

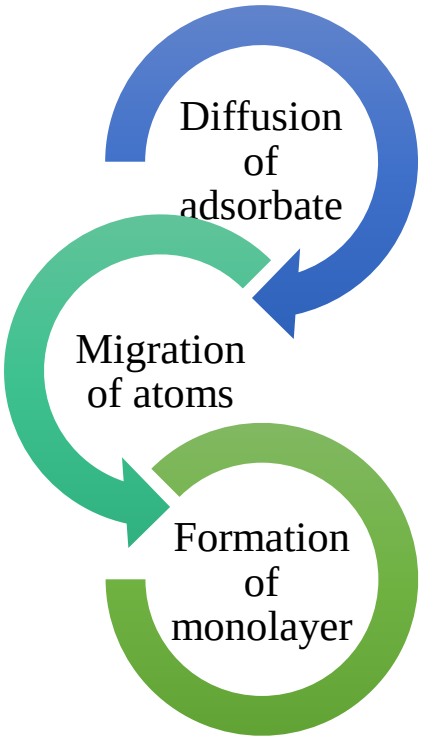

Figure 3: Mechanism of Adsorption

1.6 Adsorption process modelling

In order to find out elimination effectiveness of the material to be adsorbed, adsorption's mechanism of modelling can be used. By using adsorption isotherm and adsorption kinetics adsorption modelling can be applied. [32]

1.6.1 Adsorption isotherms

From the solution aggregation, amount of the adsorbed element can be calculated with the aid of isotherm models at fixed value of temperature. The adsorbent's adsorption potential is calculated through adsorption isotherm models. In liquid phases most frequently utilised isotherm models are Freundlich and Langmuir isotherm models.

In order to draw a design for experimental data and to evaluate it on the basis of isotherm models, and to calculate a divergance between isotherm models and calculated data, adsorption isotherm helped a lot. Furthermore, types of processes taking place at adsorbent surface, capacity of adsorbent and nature of adsorbate (monolayer or multilayer) has been evaluated easily with the aid of adsorption isotherms. [32] [33]

1.6.1.1Langmuir isotherm

Only in case of homogeneous adsorption Langmuir isotherm model will be applicable. Where all adsorbate atoms, ions and molecules had to possess equal sorption activation energy in order to homogenously adsorb on the outside. The sustained type of Langmuir isotherm is mentioned as;

$$\frac{Ce}{qe} = \frac{Kl}{qm} + \frac{Ce}{qm}$$

- "Ce" is the concentratin of adsorbent at equilibrium (mg/l)
- "Kl" is the constant of Langmuir
- "qm" maximm amount of adsorbent for monolayer (mg/g)

In accord with the model of Langmuir isotherm metal ion will adsorbed chemically, and all active sites should grip only one adsorbate. [34]

1.6.1.2Freundlich isotherm

Freundlich adsorption isotherm is the main model for multifaceted adsorption and heterogenous surfaces. Its linear form is mentioned as;

$$\log qe = \log Kf + \frac{1}{n}\log Ce$$

- "Kf " is the Freundliceh's constant
- "n" is the Freundliceh's exponent.

Here, a graph of log "qe" vs log "Ce" will allow the constant and exponent "n" to be resolved easily. [35]

1.6.2 Adsorption kinetics

The rate of reaction basically depends upon the reactant's concentration which is predicted by kinetic equations of the reactants, which are calculated experimentally by using assembled data from the experiment. Valuable information and mechanism of the reaction can be obtained with the help of adsorption kinetics. [30] The overall estimation of the mechanism of adsorption is decided from the aid of pseodo-first-order and pseodo-second-order reactions. [33]

1.6.2.1Pseudo-First Order

The lagergren Pseodo-first order kinetic model of adsorption mainly define the solid and liquid adsorption system. This model is based on equation:

$$\ln(qe - qt) = \ln qe - k_1 \mathrm{t}$$

- "qe" is absorbent adsorbed at equilibrium (mg/g)
- "qt" is adsorbent adsorbed at time 't' (mg/g)
- "k_1" is the rate constant of pseodo-first order (l/min)

Whereas "e" is an exponential function. [36]

1.6.2.2Pseudo-Second Order

In order to illustrate the kinetics of the adsorption, pseodo second-order model can be utilized effect fully. Its sustained form is represented as:

$$\frac{t}{qt} = \frac{1}{k_2 q_e^2} + \frac{t}{qe}$$

- "qe" is the adsorbad amount at equilibrium (mg/g)
- "qt" is the adsorbad amount at time 't' (mg/g)
- "k_2" is pseodo second rate constant order (g/ (mg. min) [37]

Chapter 2-Literature review

Heavy metals can not only pollute the water reservoirs but are also harmful for the biological communities so, the matter of elimination of heavy metals ions from the unusable water is of very high importance. In nature most heavy metals possess particularly high degradability and high toxicity. [38] In order to save human lives, animals and plants from a serious threat of discharge of heavy metals into the environment, their concentration needs to be reduced to an acceptable level or they need to be converted into less toxic chemicals. Even in trace amount heavy metals like chromium, arsenic, nickel, cadmium, iron, mercury, zinc, copper, cobalt, lead, bismuth and titanium have been considered as poisonous and toxic for human health. Main sources of the origin of these heavy metals are domestic effluents, pharmaceutical sewage, foundries and smelters, mining, chemical manufacturing, battery manufacturing and electroplating industries etc. [39]

2.1 Waste water treatment

So far, there are numerous water treatment processes and methods like precepitation, evaporation, solvent uprooting, ion exchange, reverse osmoses and membran filtration etc. which had been utilized repeatedly for particular elimination of heavy metallic ions from the waste watery and drinking water. Almost all of these processes possess some major flaws that are production of secondary waste materials, high cost processes, low efficiency and time taking processes. [40] [41] [42] hence, recently nano-techniques have been used frequently in order to solve these problems. In these techniques nanoparticles and especially magnetic Fe_2O_3 nanoparticles have attracted much attention. [43]

Because of excessive collection of objects proportion and finite size effect of nanoparticles it had been believed about their adsorption potential for heavy rock ions removal is quite high. Moreover it's easier to separate heavy metal rock ions from loaded magnetic adsorbent with the assistance of an outside applied magnetic field. So in this scenario, Fe_2O_3 is highly recommended for water purification applications. [44] [45]

2.2 Iron Oxide Nanoparticles

Iron oxids are basically chemical composites which are formed of mainly, iron and oxygen. It has seventeen well known other iron oxides and oxy hydroxides that exists naturally. Three main oxides of the iron are iron (II) oxide (FeO), Iron (III) oxide or ferric oxide (Fe_2O_3) and iron (II, III) oxide (Fe_3O_4). Among these oxides the best known oxide is rust, which is a form of Fe_2O_3. [46] [47]

Fe_3O_4 naturally occurs as the insentient magnetite. It consists of both Fe (II) and Fe (III) ions and occasionally it is composed as iron oxide · Fe_2O_3 Black powder is another name of iron oxide. Usually it shows permanent magnetism and hence it is known as ferromagnetic material in nature. [48] The large scale use of Fe_3O_4 is as a black pigment powder which is the only reason why it has been synthesized in the laboratory rather than extracting from minerals which occurred naturally. While by changing the method of synthesis we can vary its shape and particle size as well, according to our need. [46]

Fe_3O_4 possess a counter spinel cubic system, which comprises of a firmly united cubic lines of oxid ions and entire Fe^{2+} ions settled at center of the octahedral spots while Fe^{3+} ions have distributed over the leftover octahedral spots and the tetrahedral spots uniformly. Moreover, both FeO and Fe_2O_3 have alike close packed cubic structure just like Fe_3O_4. The electrical conductivity of the Fe_3O_4 is notably higher than Fe_2O_3.

In Fe_3O_4 the electron rotation of Fe^{2+} and Fe^{3+} ions are coupled in the octahedral spots whereas the electron rotation of the Fe^{3+} ions are also coupled in the tetrahedral sites but both spins are antiparallel to each other, because of which ferromagnetic nature of Fe_3O_4 appears. [48] Iron oxide particles having diameter in the range of 1 to 100 nanometers are known as iron oxide NPs. Two major types of iron oxide NPs are magnatite Fe_3O_4 and maghamite Fe_2O_3. [49]

2.2.1 Phases of iron oxide nanoparticles

Iron oxid contain sixteen refined phases. Which are as following;

- Oxides for example Hematite, Magnetite, Maghemite and FeO alpha phase
- OH for example Iron(II) OH, Iron(III) OH and Bernalite

- Oxy-hydroxides for example Feroxyhyte, Lepidocrocite, Geothite and Akaganetite

These compounds owned some particular properties such as distinct shades, low solubility and trivalent state. [46]

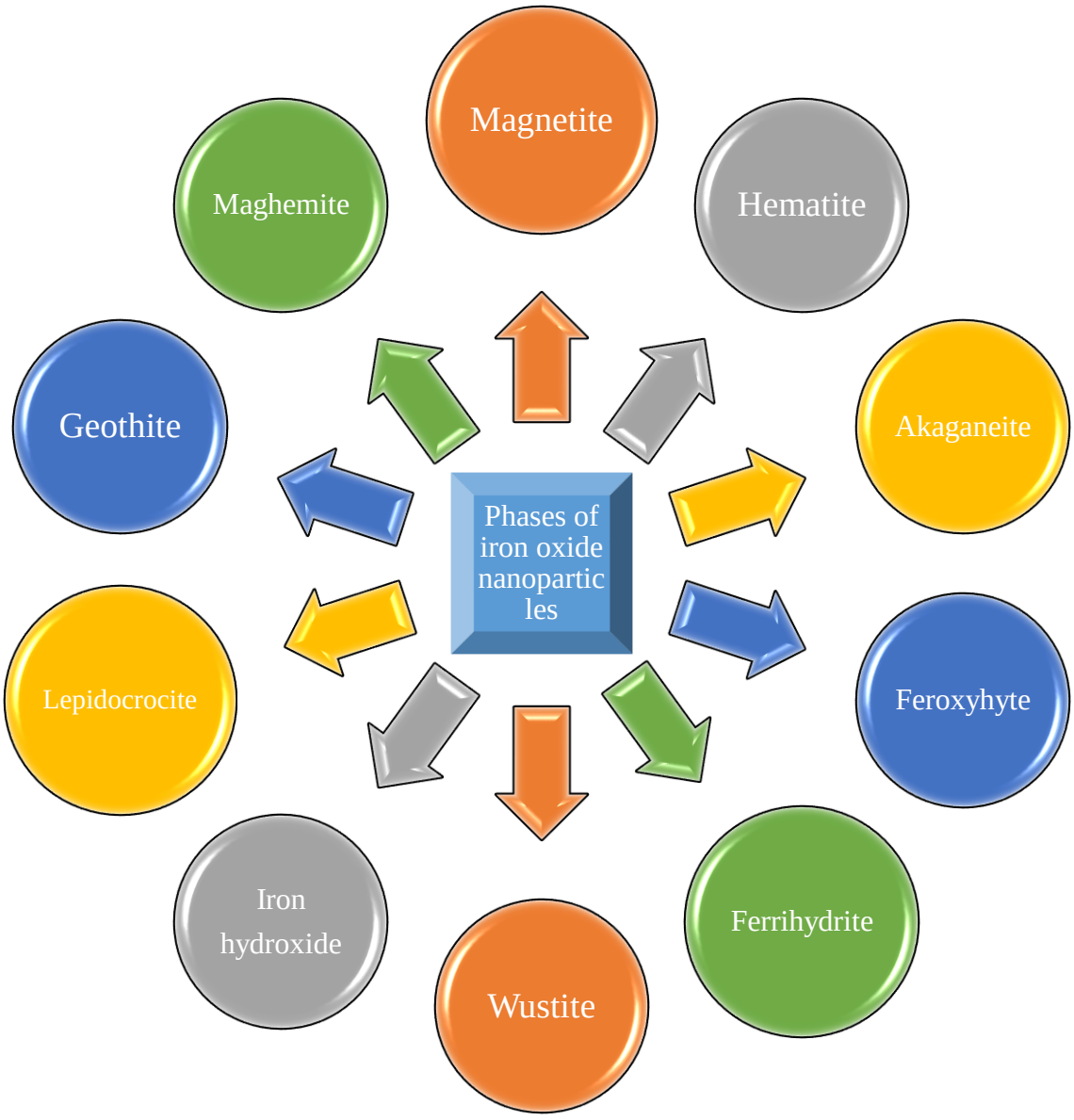

Figure 4: Phases of iron oxide nanoparticles

2.2.2 Applications of Iron Oxide Nanoparticles

Fe oxide NPs had surely been largely utilized as highly energetic catalysts in various acid/ base reactions and oxidation/reduction reactions. [50] Iron oxide based compounds have been considered as most efficient and inexpensive materials as an environmental catalysts. In recent researches it has been proved that iron oxide nanoparticles are more productive than traditional large sized iron oxide due to their high collection of objects ratio and high susceptibility. [51] [52]

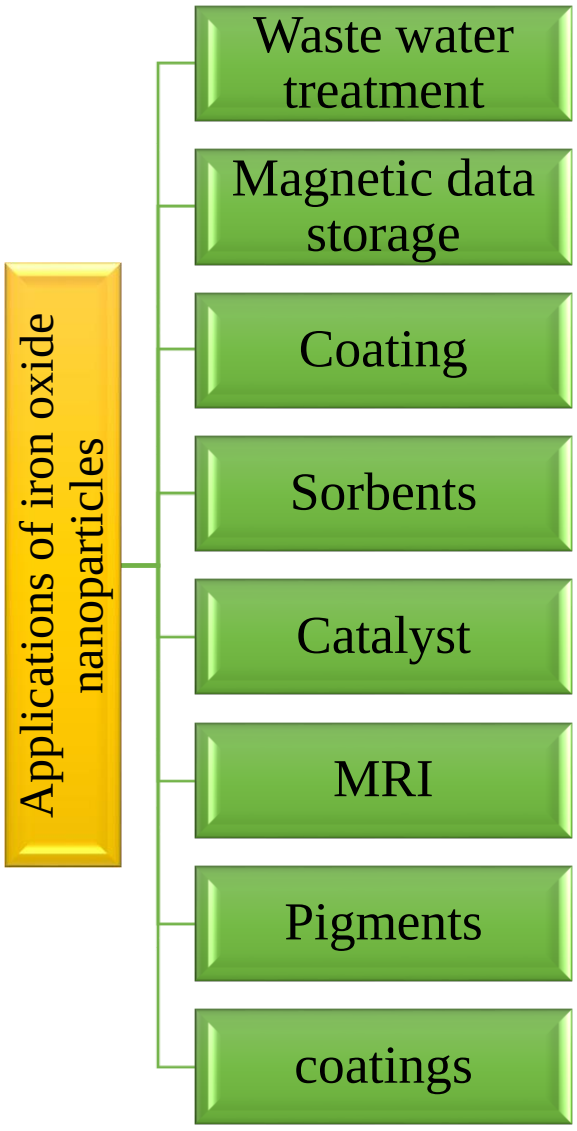

Figure 5: Applications of iron oxide nanoparticles

2.3 Synthesis of Iron Oxide Nanoparticles

Iron oxide nanoparticles can be formed by countless methods which had been utilized so far for it and the final product contains mixture of different phases. Generally particle characteristics of the iron oxide could be controlled through the usage of organic processes like co-precipitation and hydrothermal synthesis. But by using discontinuous and batch type processes large scale and fast production of the iron oxide nanoparticles is not possible. [53] We have numerous chemical, non-living and pathobiological methods for the synthesis of required nanoparticles to achieve proper hypnotic characteristics, shape along with the size of particles.

2.3.1 Solvothermal Method

Solvothermal is such a type of method, which is used for the synthesis of all types of chemical compounds. In terms of conducting synthesis in a stainless steel autoclave, this process is very similar to hydrothermal process. The most important dissimilarity in it is the usage of precursor mixture which is not aqueous, which is not necessarily true. [54] Solvothermal method provide us control over shape, definite size control and check over crystallinity of metallic nanoparticles or other nanostructured products. These features can be altered by varying specific parameters like time and temperature of reaction, solvent and surfactant type and particularly precursor used in the reactions. [55]

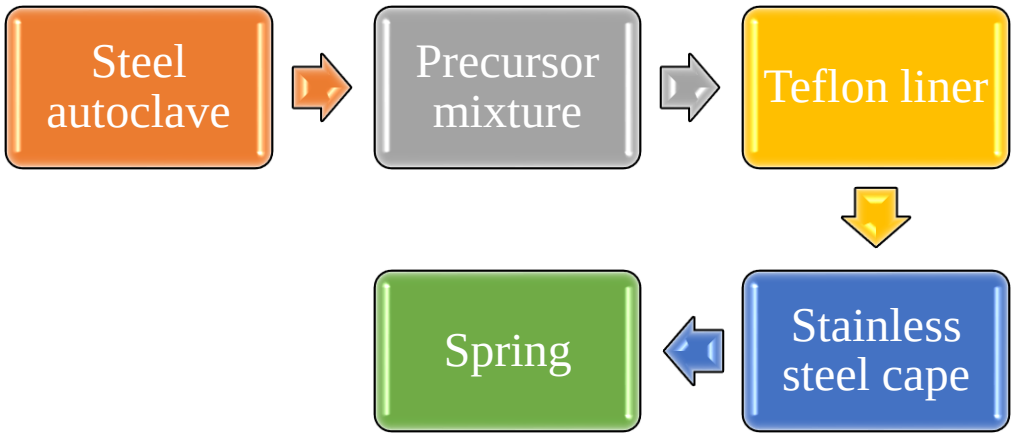

Figure 6: Flow chart for Solvothermal method

2.3.2 Thermal Decomposition Method

Thermal decomposition is basically a synthetic decay which is due to high temperature and it is also known as thermolysis. Usually heat is required in this method in order to smash electrovalent bonds in the compounds, which undergoes decay and the response will be exothermal in nature. [56] It particularly the most effectual way to synthesize small size magnetic nanoparticles, which will give us ultimately fine adjustment of particle's diameter. [57] Usually it can be achieved by dual ways that is "heating-up" and "hot-injection". The constant increasing temperature of pre-blended solution of precursor compounds, solvent and surface active agents at a particular temperature represents the heating-up process. At this temperature nanoparticles will start growing and clustering. [58] [59] whereas, introduction of analytes into a hot surfactant solution is known as hot-injection process, which gives us controlled growth, fast and homogeneous nucleation. In nut shell, both processes are based upon same concept which is heating. [60]

2.3.3 Hydrothermal Method

One of the utmost usual technique for the preparation of NPs is hydrothermal process, which is actually a solution reaction-based technique. Various types of nanomaterials can be produced with the special aid of this approach. The formation of the NPs can happen in a vast span of temperature that is from very high temperature to room temperature in hydrothermal technique. Successively to manipulate the surface structure of the NPs, depending on the reactants vapor pressure, either high-pressure or low-pressure environment can be used. There are various notable advantages of hydrothermal method over other methods. Which are

- Generation of nanoparticles which are unstable at higher temperatures.
- Production of nanoparticles with minimal loss of byproducts, particularly at high vapor pressure.
- Controlled synthesis of nanomaterials via multiple chemical reactions. [61]

2.3.4 Co-precipitation Method

Co-precpitation is a facile and appropriate method to synthesis iron oxide NPs (one of two Fe_2O_3 or Fe_3O_4) from aqueous salt solutions of Fe^{2+} /Fe^{3+} with the incorporation of base. It could happened under either at inert atmosphere or at optimized temperature. Different parameters like shape, size and configuration of the magnetic NPs turn on upon following variables:

- Reaction temperature and other conditions
- pH value of the reactants
- Ionic strength of the reactants used
- Fe^{2+} /Fe^{3+} ratio
- Types of salts used like chlorides, sulfates, nitrates, carbonates etc. [62]

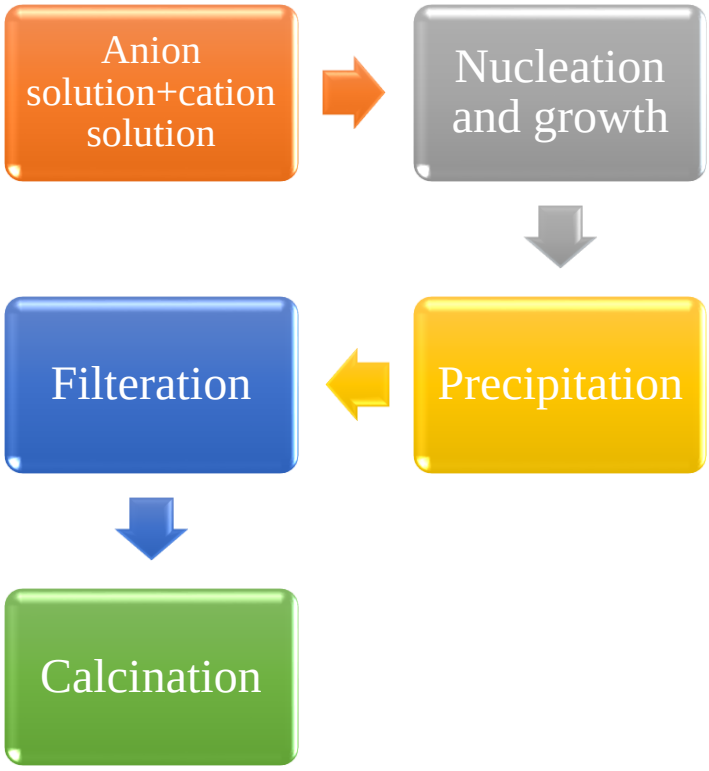

Figure 7: Flow chart for Co-precipitation method

2.3.5 Polyol Method

Uniform magnetic nanoparticles can be produced easily by using this method at moderate temperature. This method referred to few precursor compounds like oxides, nitrates and acetates, where they either lies in dissolve state or in suspended state. It is an adaptable synthesis method which is utmost suitable for the generation of huge clusters of iron oxide nanoparticles having vast range of possible sizes. Such type of characteristics can be defined on the basis of reaction temperature, reaction time, precursor used, type of solvent and surfactant used. [63] [64] In order to obtain Nan crystalline compounds or alloys polyol is a really useful technique. [64]

2.3.6 Sol-gel Method

This is a particularly well-established and encouraging approach for the formation of high-grade nanoparticles of rock metal oxides and metal oxide composites. Shape, size, texture and surface features of the nanomaterial can be efficiently controlled with the help of this technique. Generally sol-gel technique can be explained in five major steps; Hydrolyses, polycondnsation, aging, drying and thermal dbreakage. [65]

Step 1: Hydrolysis

Either water or alcohol is used usually for the hydrolysis of metal alkoxides. In order to produce matel oxide nanoparticles, oxygen is an essential component which is provided by water or alcohol. In auueous sol-gel method water is utilized as reflection medium and in nonaqueous sol-gel method alcohol is used as reaction medium. An acid or base can also be used for the hydrolysis of precursors. Chemical reaction for hydrolysis process is:

$M\text{-}OK+H_2O \rightarrow MOH+KOH$ (Hydrolysis)

Here M=metal, K=alkyl group (C_nH_{2n+1})

The quantity of water had a great impact on the gel formation in this step. [66]

Step 2: Condensation

In this step water/alcohol molecules are removed and condensation of consecutive molecules occur along with growth of polymeric networks. Condensation take place through two processes oxolation and olation. Oxolation is such a type of process in which (-O-) oxo group is formed between two metals and olation is such a type of process in which (-OH-) hydroxyl group is established in the middle of two metals. Chemical process for condensation process is:

M-OH+YO-M → M-O-M+YOH (Condensation)

Here M=metal, Y=H or alkyl group (C_nH_{2n+1})

In this step viscosity of the solvent increases and we will get spongy structure along with liquid phase which is known as gel. [67] [68] [69]

Step 3: Aging

Structural properties of the gel will vary in this step. During this step first condensation of the solution occurs then re-precipitation of the gel solution starts. Eventually porosity will decreases in this step.

Step 4: Drying

There are different processes of drying like thermal drying, freeze drying, atmospheric drying and supercritical drying. Different kind of gel's structure is associated with each type of drying. Drying at high temperature may increases the density of the gel and convert it into xerogel which exhibits low surface area and volume of pores. [70] At high temperature usually shrinkage of gel is experienced. [71] Whereas, while supercritical drying aerogel is obtained with high surface area and pore volume. At supercritical drying conditions gel network remain unflawed. In freeze drying solvents are dried by freezing and at the end cryogel is obtained, in which little gel shrinkage is noticed. Relative humidity is an important factor which needs to be considered while drying nanomaterial. Relative humidity can control the stability of the nanoparticles. [72]

Step 5: Thermal decomposition

Finally thermal treatment is conducted to remove the remaining water or alcohol molecules from the required sample. In controlling the pore size and sample density calcination temperature plays an important role in this step.

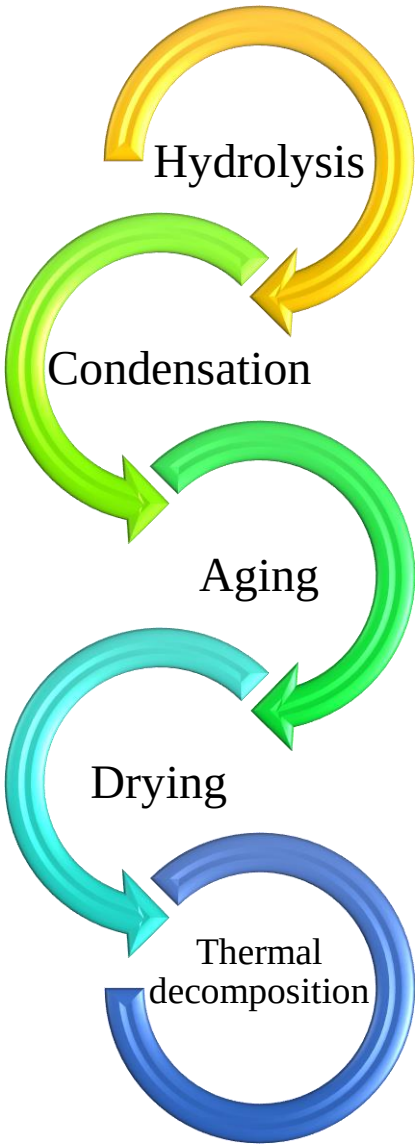

Figure 8: Steps involved in Sol-gel method

2.4 Iron oxide coated materials

To get an efficient adsorbent not only its cost aspect is important but adsorption capacity is also very important and needs to be considered. An adsorbent with maximum surface area and available active sites will exhibit maximum adsorption capacity. In some cases it is worth noted, that porosity of the material used will have an immense impact upon the extent of the adsorption of adsorbent. So an ideal adsorbent need to have following properties:

- immense exterior area
- Presence of huge number of active sites on surface
- Resistive to unfavorable environmental conditions
- Chemically stable
- Renewable and can easily separate from treated water [73]

It has been confirmed from the previous study, that surface functionality or modification of nanomaterial shows a significant role in the enhancement of adsorption efficiency. Moreover presence of various substructures on the surface will avoid unnecessary oxidation of the material and the material will become more stable chemically and hydrothermally. [74]

2.5 Chitosan-Iron oxide hybrid beads

Lately, Chitosan (CS) has been considered as a novel polymeric material, which has been widely used in many applications due to its unique characteristics. It has few distinctive properties for example biocompatible, nontoxic, biodegradable etc. [75] Moreover because of some other special unpredicted properties of chitosan like low specific gravity, poor mechanical strength, poor solubility, agglomeration etc. it became more suitable for adsorption purpose. Hence it has been widely used in environmental pollutant removal based applications for example for heavy metal removal or dye removal from polluted water, it could be industrial or drinking water. [76] [77] so in that scenario, successively to upgrade these unpredicted properties of chitosan, it could be used in the combined state with other materials.

Iron oxide nanoparticles can be coated with biomaterials like chitosan in order to enhance their chemisorption ability. Chitosan is an abundantly available biocompatible and nontoxic polymer, which is easily obtained from crabs, lobsters and shrimps etc. Up till now it has been observed that pure chitosan is more productive in its performance than its chitin (precursor). [78] Chemisorption of the toxic heavy metal ions will be facilitated by cause of existence of chitosan along with NH group on it and ultimately, these metal ions will be eliminated from waste water. [79]

Moreover, iron oxide nanoparticles will become less toxic and environmental friendly after chitosan coating and then could be easily used for heavy rock metal ions elimination from drinking water. In this way we can get a cost effective method by using hybrid iron oxide nanoparticles and chitosan composites, which can be specifically used at large scales in water pollutant removal applications. [80]

Chapter 3- Materials and Methods

3.1 Chemicals required

A highly viscous chitosan used for preparation of beads was procured from sigma Aldrich along with a moleculer weight of 500,000 and 84% degree of deacetylation. Acetic acid (glacial 99-100%), Sodium hydroxide, Iron (III) Chloride Hexahydrate ($FeCl_3.6H_2O$), Iron(II) Chloride Tetrahydrate ($FeCl_2.4H_2O$) and Chromim(VI) Oxide (K_2CrO_4) were purchased from Merck. Ethylene glycol (MW 62.07) was brought from sigma Aldrich.

3.2 Synthesis of Magnetic nanoparticles

The amalgamation of Fe_2O_3 nanoparticls (NPs) has been done by using sol-gel method. In this process Iron (III) chloride haxahydrate (4g), Iron (II) chloride tatrahydrate (3g) and ethylene glycol (100ml) were mixed with each other in a beaker on hot plate at 45˚C under continuous magnetic stirring to form a homogeneous mixture. After continuous stirring for 2 hours under 50˚C temperature gel like compound will be obtained, which will hardened with in few hours at same previous temperature. Then this hard gel will be dried on hot plate for another 24 hours at 150˚C. Now grind it using mortar pestle until fine powder is obtained. Finally, in order to dry nanoparticles completely put them in vacuum oven for 4 hours at 100˚C. Fe_2O_3 magnetic nanoparticles possess a special property that, they can be separated from any medium anytime with the help of an externally applied magnetic field.

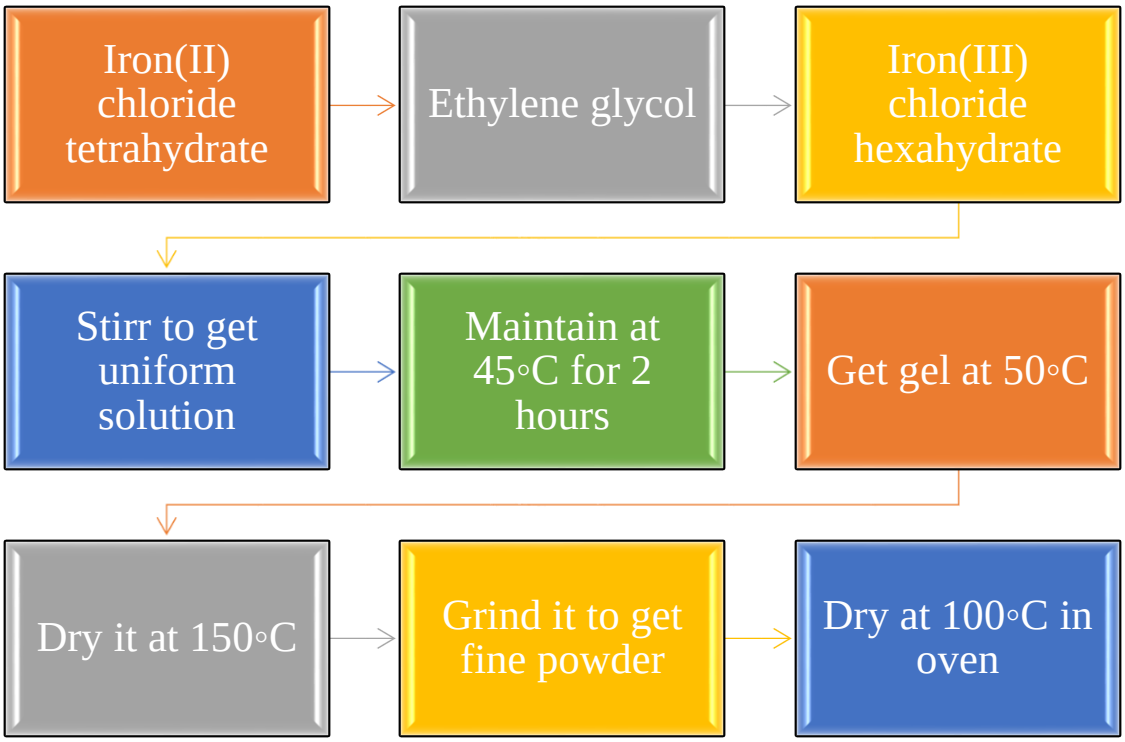

Figure 9: Block diagram of Synthesis of Iron Oxide Nano particles

3.3 Synthesis of Iron oxide embedded chitosan beads

Iron oxide embedded chitosan beads (IECB) were synthesized by using embedding method. Where as, iron oxide NPs were prepared by using method of Sol-Gel prior to this. In the synthesis of hybrid beads mix 2.6% v/v acetic acid of 50ml solution with 5 grams of chitosan under constant stirring (450rpm) for 4 hrs. After getting viscous transparent solution, add 1.5g of Fe_2O_3 nanoparticles in it and stir it again to obtain viscous homogeneous solution. For deaeration, sonicate this solution at room temperature for 5 minutes. Now the resulting slurry of Chitosan-iron oxide solution was added drop wise with the help of a syringe into 1mol/L NaOH solution under continuous stirring. Millimeter size beads will be assembled in the NaOH solution. Then hybrid chitosan-iron oxide beads were taken out from the solution of NaOH and bathed in water many times until, neutral pH of the filtrate is obtained. Finally, beads will be dried by using an oven at 65˚C for 4 hours.

3.4 Beads with different compositions

Table 2: Beads with different compositions

Sample	**Chitosan (g)**	**Fe_2O_3 Nanoparticles (g)**
Bead 1	2g	1.5g
Bead 2	3g	2g
Bead 3	4g	2.5g

Among these 3 compositions bead 3 gave best adsorption efficiency.

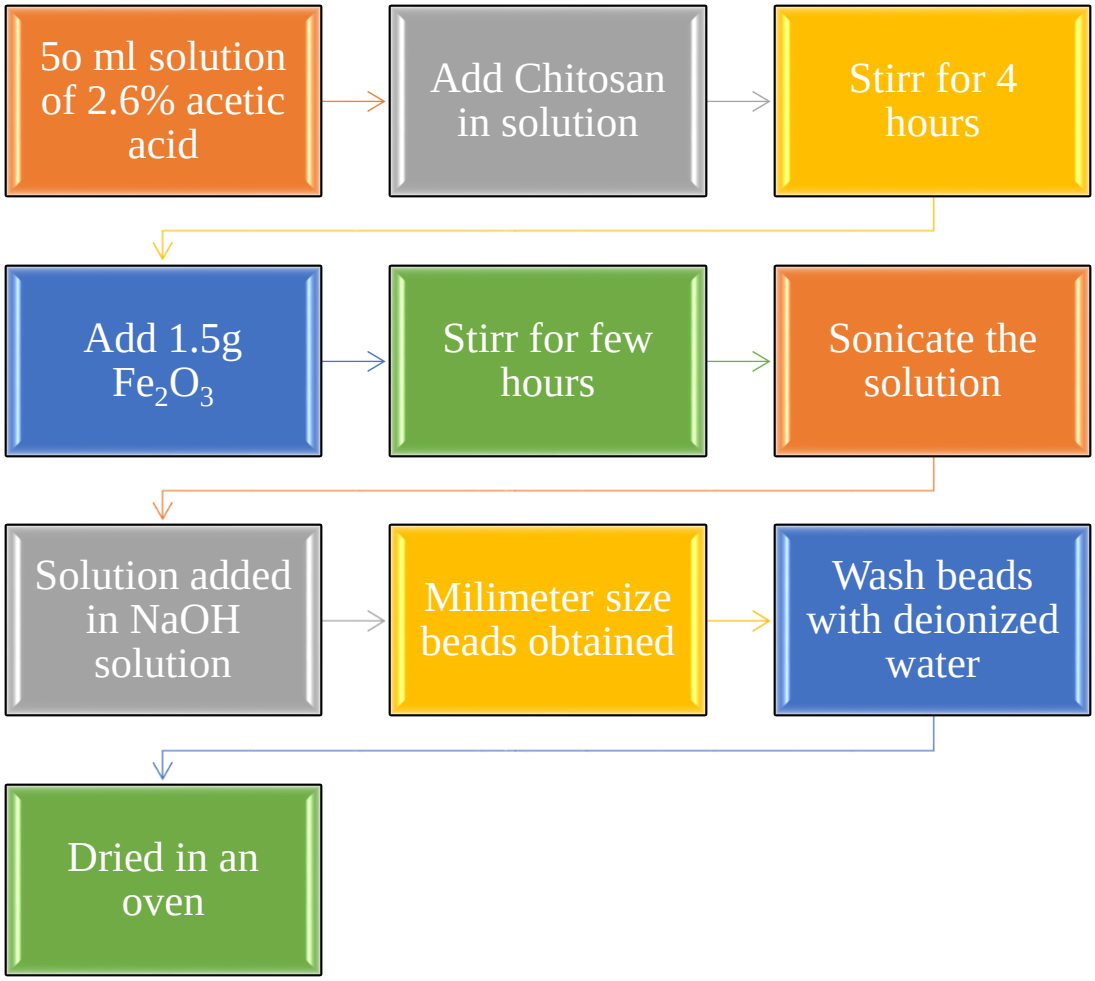

Figure 10: Block diagram of Synthesis of Hybrid Chitosan-Iron Oxide beads

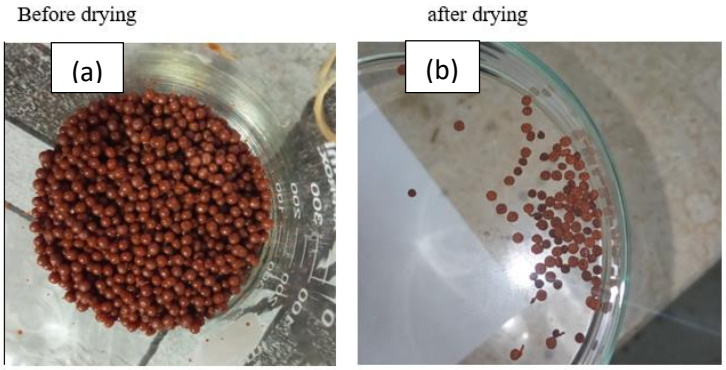

Figure 11: Bead 1 (a) before and (b) after drying

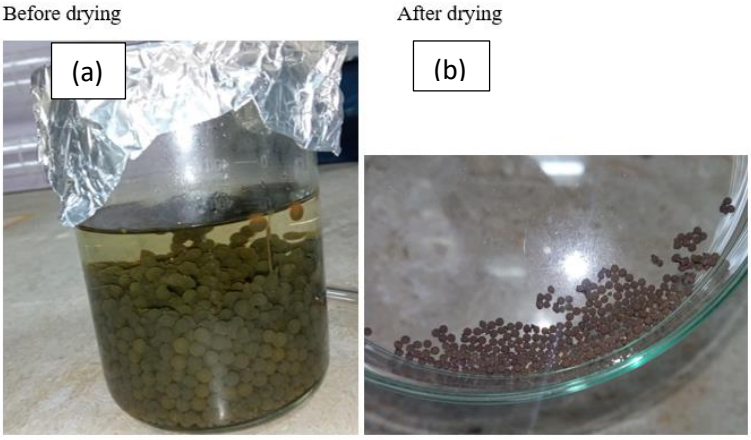

Figure 12: Bead 2 (a) before and (b) after drying

Figure 13: Bead 3 (a) before and (b) after drying

3.5 Characterization techniques

In order to get the characterization of Fe oxide NPs and hybrid beads following techniques were used:

- Contact Angle
- Thermogravimetric Analysis (TGA)
- Scanning Electrone Eicroscope (SEM)
- X-Ray Diffraction (XRD)
- Fourier Transform Infrared (FTIR) Spectroscopy
- Vibrating Sample Magnetometer (VSM)
- Brunauar-Emmatt-Teller (BET)
- UV-Vis Spectroscopy

3.5.1 X-ray Diffraction

Now a day it is a common method, which is utilized to determine the crystal structure of an element along with its interplanner spacing. The phenomenone of constructive interference of monochromatic spectrum is involved in X-ray diffraction. Cathode ray tube is used for the formation of X-rays then after filteration monochromatic radiations will be obtained, which will be concentrated with the help of a collimator. Finally these X-rays will be directed toward the specimen. When incoming rays will interact with the specimen then constructive interference will occur and diffraction will occur when Bragg's law will be satisfied.

$$n\lambda = 2dsin\theta$$

X-ray diffractometers comprises of three basic components. Which are as following

- An X-ray tuba
- A specimen holder
- An X-ray detector

This technique is an excellent, modern and un-infectious characterization method. Which has been globally used for the detail analysis of many materials like metals, nonmetals, plastics, semiconductors, ceramics, films and fibers etc. Sample can be used in powder form for X-ray diffraction. Very minimal sample preparation is needed for this technique. [87]This technique's (XRD) design of α-Fe_2O_3 along with IECB were acquired at optimal warmth by D8 Advance, Bruker ASX, utilizing CuKα radiation (λ=1.54 Å) in the range of $2\theta=20^0$-90^0, and a sampling speed of $0.02s^{-1}$.

3.5.2 Scanning electron microscope

In SEM concentrated ray of electrons is used to create the images of specimen, by examining the surface of the sample. Various signals will be produced when incoming electrons will interrelate with the atoms of the surface. Along with features of the surface, we can check the composition of the sample as well with the help of SEM. During raster scan, it has been observed that electron beam excite the secondary electrons which emit from the surface atoms and a detector detect them. A highly efficient scanning electron microscope usually gives resolution better than 1 nm. In scanning electron microscope samples can be analysed under different conditions like high vaccum, low vaccum and under variable pressure or temperature conditions. Samples scanned under SEM needs to be small and conductive enough so that they can be adjusted on sample stage easily and can be analysed under high vaccum atmosphere. [82]

SEM images were get hold with JSM 6700I Scaning electron Microscope in order to investigate the patterning and suface construction of the bed at different magnifictions at optimum heat. The dried sample was placed on a bras holder and bombarded with a covering of gold particles in vaccum. For secondary image 20kV accelerating voltage was used.

3.5.3 Fourier-transform infrared spectroscopy

A high resolution spectral data over large range of spectrum can be obtained with the help of FTIR spectroscopy. Absorption or emission spectrum of infrared light of gas, liquid or solids can be equired from this technique. In order to transform the crude data into the genuine spectrum, fourier transform (a maths procedure) is used. [84] FTIR

spectrum was noted down in Perkin-Elmer-283B FTIR spectrometar across the waving span of 3700-450cm^{-1}.

Instead of using Monochromatic illumination at the smaple, this method uses a light of various frequencies at the same time and absorbance of light by the sample is calculated. Moreover, to get second data point, different frequency combinations can be use in this technique. In the same way, this process will repeat many times in the same time interval. In the end, at the back end of the computer all this data will be analysed quickly and corresponding each wavelength, absorption of spectrum will be measred. [85]

3.5.4 Contact Angle

Angle at which vapour-liquid interface connect the solid surface is known as contact angle. This phenomenon can be demonstrated by placing a tiny droplet of water on the horizontal surface of solid. In this case by using young-laplace euation shape of the droplet can be decided and boundry conditions can be determined with the help of the angle between solid-liquid interface. Contact angle goniometer could be used to determine the contact angle. Basically contact angle give us information that either the force of attractiveness between the atoms of the droplet for each other is stronger or it is stronger between droplet molecules and surface molecules. Approximately 0◦ contact angle will be obtaned if the molecules of the droplet will be completely attracted toward the surface molecules. Contact angles up to 90◦ shows less hydrophilic solids. Whereas hydrophobic surfaces exhibit angle greater than 90◦. [81] In order to get the measurements of contact angle a drop of liquid is placed on the bead then with the help of a camera (with a lens system), which is back lit with a flas light an image is taken. At last imagej software is used to analyze this drop image and the value of contact angle can be calculated.

3.5.5 Ultraviolet–visible spectroscopy

This technique is described as absorbance spectroscopy in which EM spectrum contain visible and ultraviolet portions. Distinguished colours of the chemicals involved have been obtained by the absorption or reflectance of the visible light in UV-Vis spectroscopy, and electronic transitions of atoms and molecules can observed in it. According to the working primciple of UV-Vis, bonding and non-bonding electrons can

excite to the higher antibonding molecular orbits in a molecule by absorbing energy in the shape of ultraviolat amd viseble light. [83]Absorbane calculations (UV-Vis) spectrum were computed via Agilant 8453 UV-Vis spectrophotometer set-up with 200-800nm wavelength.

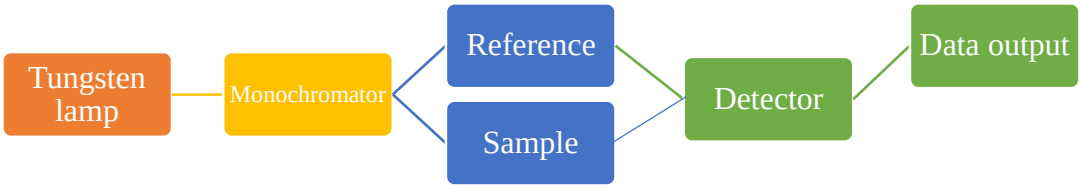

Figure 14: Schematics of UV-Vis spectroscopy

3.5.6 Tharmogravimetric analysis

Tharmal gravimetric analysis is a type of technique in which samples are thermally analysed and density of that specimen is analysed as a time's operator with the change of heat. By this technique we would be able to determine some physical parameters of the samples like adsorption, absorption, phase transitions, stability and desorption. In terms of chemical parameters thermal decomposition, chemisorption can be calculated as well. [86] this technique is mainly used for the investigation of compounds which are polymer based like nylon, polyethylene, epoxy and plastic etc. TGA was performed on dried specimens utilizing Mettler Thermal Analyser TG-50 in the optimum heat span of 25-800^{0}C with warm up rate of 10^0 C/min along with N_2 elated at 190 ml/min.

Chapter 4-Results and Disscusion

4.1 X-Ray diffraction

4.1.1 XRD pattern of Iron Oxide NPs

By detecting the attraction of black powder of α-Fe_2O_3 nanoparticles by magnet, its magnetic nature will be verified. Usually XRD technique is used for the determination of crystallite size, structure of synthesized particles and interplanner spacing etc. Figure shows the XRD pattern of α-Fe_2O_3 nanoparticles. In XRD pattern all intense peaks could be indexed with JCPDS card number 024-0072, and it corresponds to α-Fe_2O_3 formation along with Rhombohedral symmetry.These outcomes are in perfect agreement with SEM results. Main charecteristic peaks of α-Fe_2O_3 are shown at 2θ values of 24.1°, 33.2°, 35.6°, 41°, 49.6°, 54.1°, 62.7°, 64.0° corresponding to the reflection from the planes (012), (104), (110), (113), (024), (116), (214) and (300) accordingly reported in literature. [110] Moreover, some additional peaks of α-Fe_2O_3 have been observed in the pattern as well like at 2θ value of 57.8° (112) and 69.8° (208) as shown in figure 15 (b). Size of particles can be administered by manupulating the conditions of reactions like reaction temperature, agitation speed and time required for reaction,. In order to determine the crystallite size of α-Fe_2O_3 a fine scan execution needs to be done on major diffraction peak 33.2° having plane (104). Then after applying scherrer's formula average crystallite size calculated for nano particles is 14.9 nm. [116]

4.1.2 XRD pattern of Iron Oxide NPs embedded chitosan beads

Iron Oxide embedded Chitosan bead's XRD patter is shown in the figure 15 (c). It possess the main peak of chitosan at 2θ=20.9° which is because of the existence of plenty of OH and NH groups in the pure chitosan formation as shown in figure 15 (a) [117] Because of formation of a composite with α-Fe_2O_3, chitosan lost its crystalinity and intensity of the graph will decreases because of it, at the end an amporpous material will be synthesized which will be beneficial for the process of Cr (VI) adsorption. In XRD pattern of IECB, main peaks of the α-Fe_2O_3 are shown at 35.6° and 57.8°, which confirms the presence of magnetic nature in beads. Because of embedment of α-Fe_2O_3 nanoparticles into the CTS beads, repression in peaks was observed. [118]

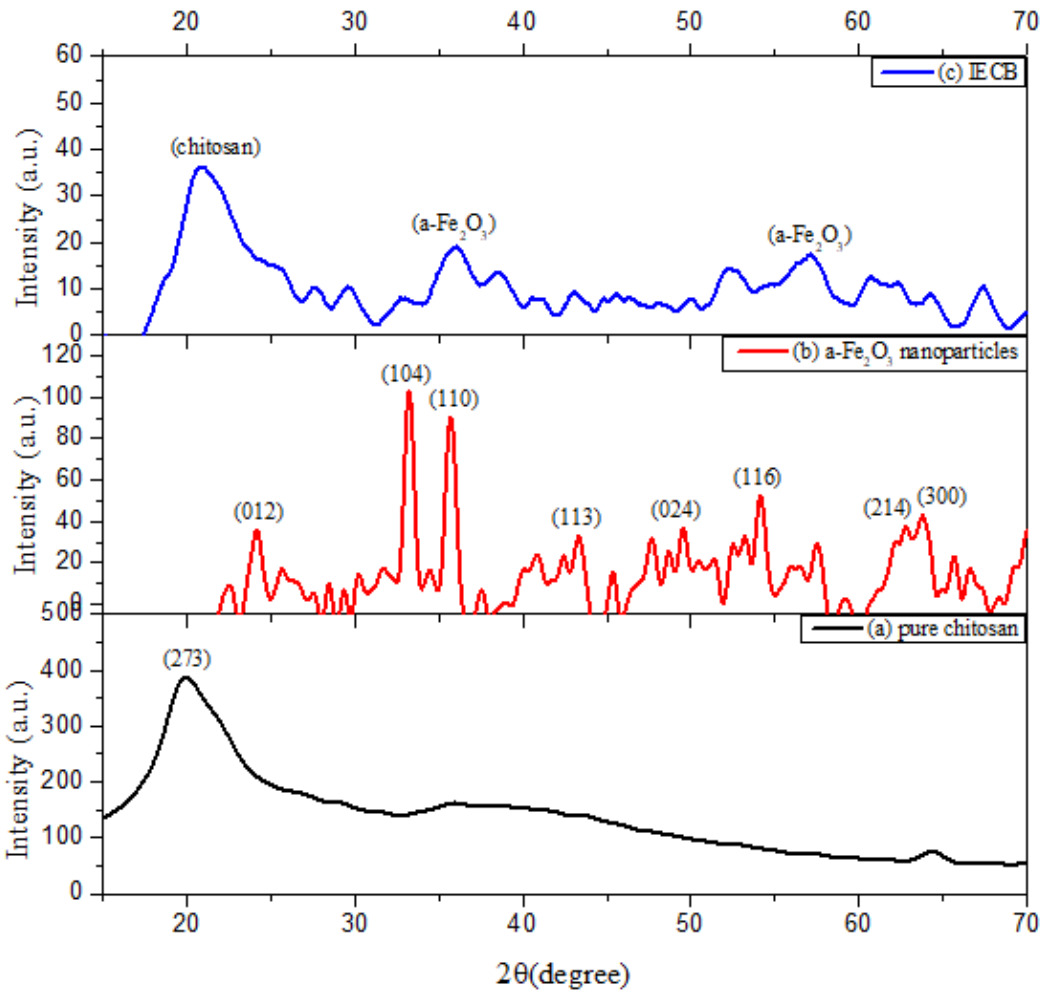

Figure 15: XRD pattern of (a) pure chitosan (b) α-Fe_2O_3 NPs (c) IECB

4.2 Scanning Electron Microscope (SEM)

4.2.1 SEM of Iron Oxide NPs

The largeness and appearance of Fe Oxide NPs synthesized by Sol Gel method was examined by SEM as shown in figure16 (a), (b) at magnification (5kx, 30kx). It has been observed that Iron Oxide NPs are rhombohedral in shape with some agglomeration. Moreover, they have uniform nanoparticles morphology and are homogeneously distributed. [109] the calculated range of the diameter of NPs is 50-80 nm and average diameter is about 70 nm. As a result of steric effect of many nanoparticles, agglomeration will occur, which is ultimately associated with the interaction of active sites upon the

exterior of Iron Oxide NPs. [110] another reason for agglomeration is the magnetic interaction created by all NPs. [116]

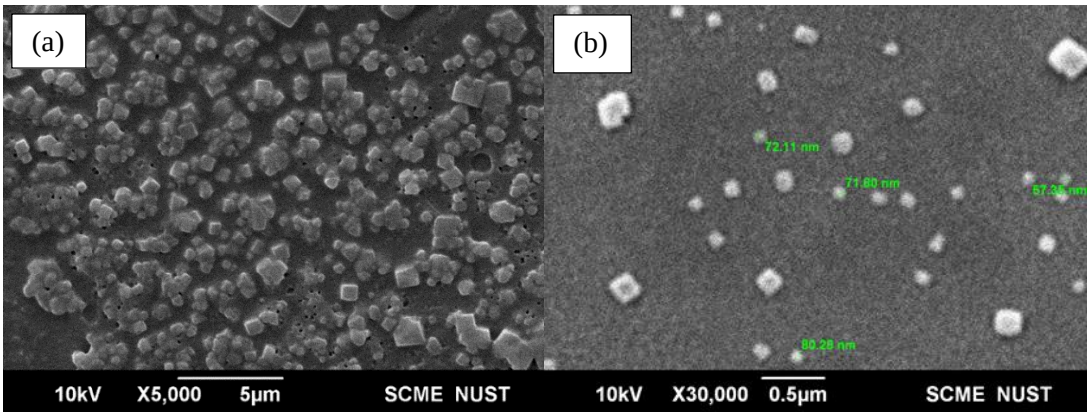

Figure 16: SEM images of Iron Oxide NPs

4.2.2 SEM of Iron Oxide embedded chitosan beads

The SEM images of IECB are shown in figure 17. It has been observed that beads have spherical shape along with quite irregular and less porous surface. The spherical bead's thickness vary from 1.47mm to 1.82mm. These results were in complete agreement that the beads were synthesized with the suspension in a mixture. [111] After addition of Iron Oxide NPs in chitosan different folds have been noticed on the surface of the beads along with white spots (α-Fe_2O_3), because of these folds huge specific area of surface and several mobile sites appeared on the outer surface. [112] this type of bead's morphology was probably because of the linkage of pure chitosan chain groups (–NH_2 and –OH) with Iron Oxide NPs. Afterwards, at the time of Cr (VI) adsorption, these groups will complex together with metal ions. [113]

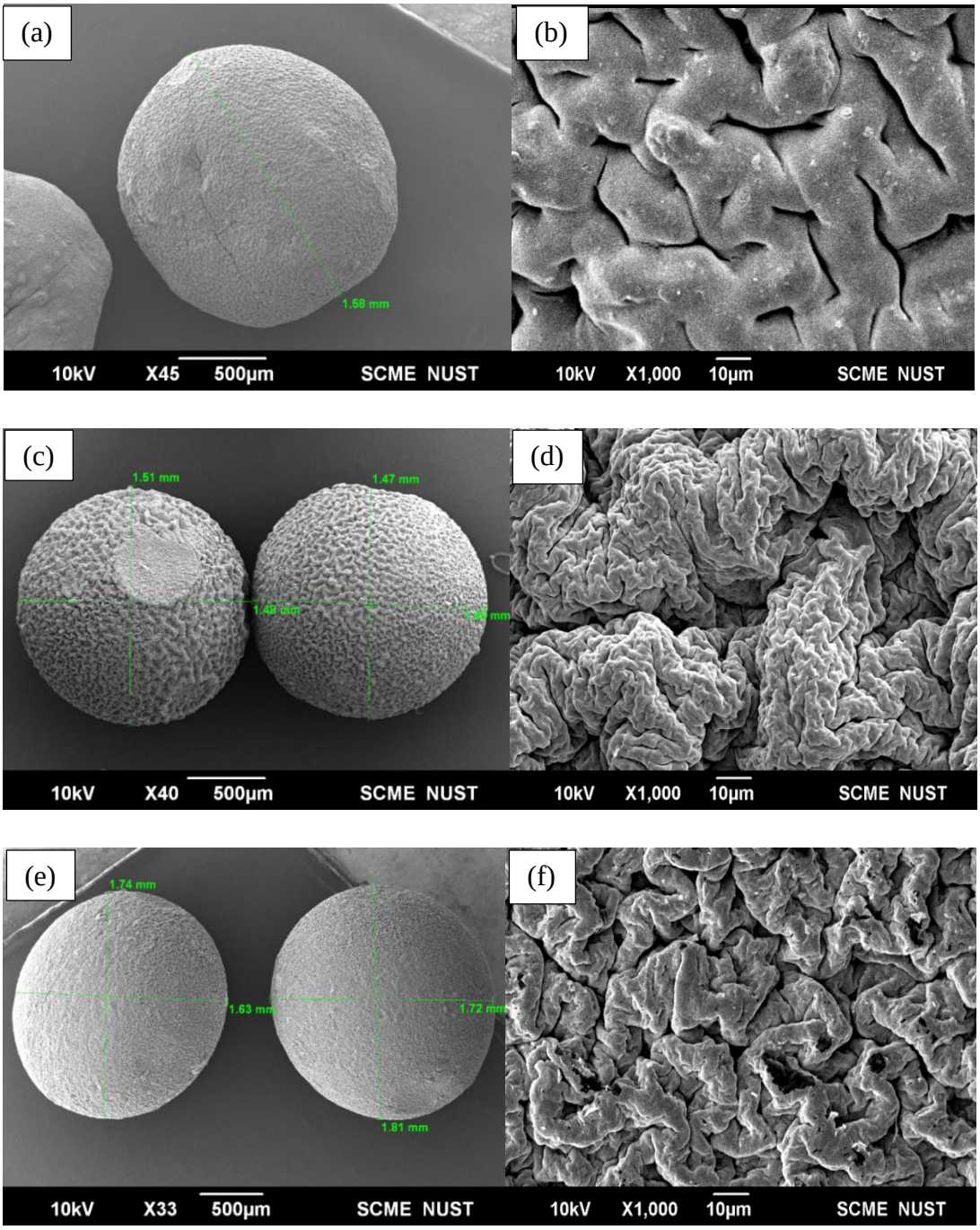

Figure 17: SEM image of IECB B1 (a) (b), B2 (c) (d) and B3 (e) (f)

4.2.3 SEM of Iron Oxide embedded chitosan beads after Cr (VI) adsorption

Scanning Electron Microscope shows the images of Iron Oxide embedded chitosan beads (B1, B2, and B3) after Chromium (VI) adsorption in figure 18. After adsorption of Chromium (VI) no distinctive variation was noticed in the surface appearance of the beads. However, small particles of Chromium (VI) attached on the surfaces of the beads can be seen clearly in all SEM images, they block the angstrom size pore structure present on the beads surfaces. [114] Moreover, a multilayered structure can be observed on the outer surfaces of the beads which proves the presence of Chromium (VI) on bead's surfaces. So in nut shell, a layer of adsorbate (Chromium) covered the adsorbent outer surface, while its internal structure remains same. [115]

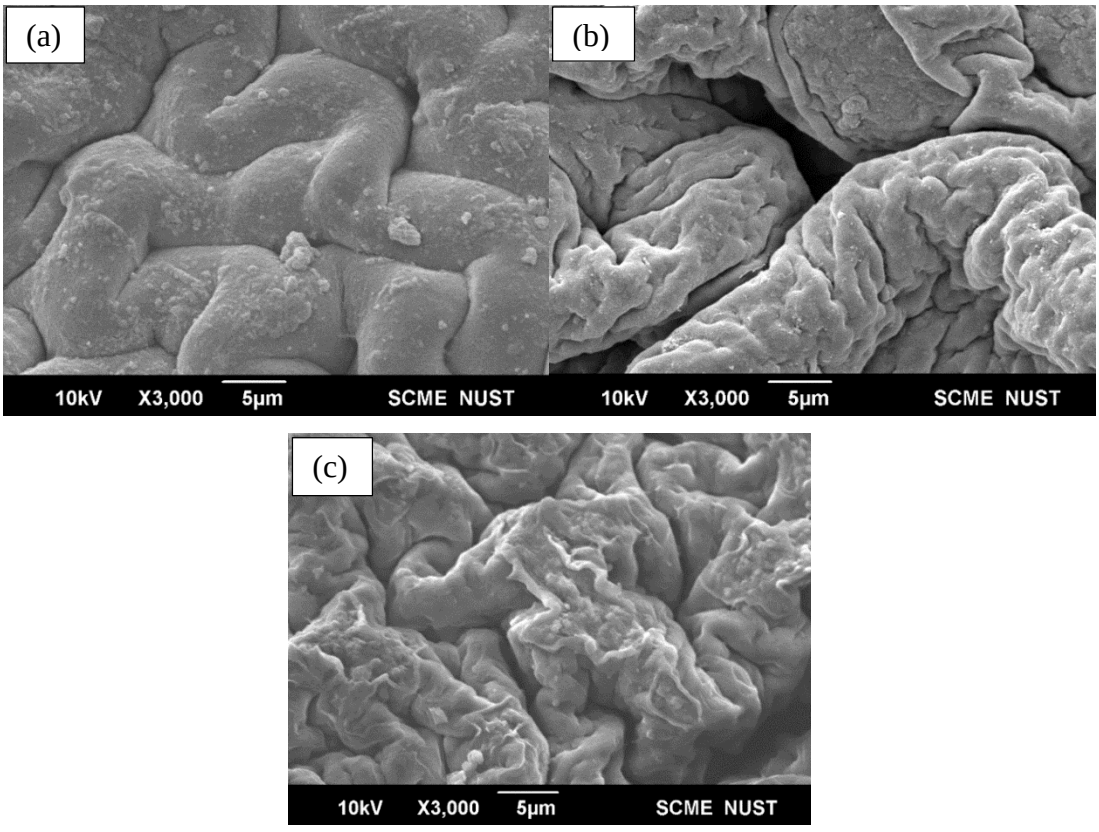

Figure 18: SEM of IECB B1 (a), B2 (b) and B3 (c) after Cr (VI) adsorption

4.3 Fourier Transform Infrared (FTIR) Spectrometer:

4.3.1 FTIR of Iron Oxide NPs:

FTIR can give details about functional groups of α-Fe_2O_3 nanoparticles. The important bands seen at 602 cm^{-1} and 556 cm^{-1} in the figure 19 (a) can present to Fe - O modes of vibration. [110] Another bend at 889 cm^{-1} refers to the C-H vibrations due to the addition of ethylene glycol during synthesis of NPs. Band at 1051 cm^{-1} appears because of the absorption of –C-O-C bonds. [119] 1370 cm^{-1} band attribute to –C-O stretching mode. Moreover because of stretching vibrations of C=C a band is seen at 1554 cm^{-1} in spectrum. Because of absorbed water, O-H stretching oscillations appeared at a wide band from (3134 cm^{-1} to 3331 cm^{-1}). [120]

4.3.2 FTIR of IECB

Normal adsorption bands of pure chitosan lies at wavenumber 3427 cm^{-1} and 1633 cm^{-1} which are linked with O - H and N-H vibrations. [121] here figure 19 (b) shows the FTIR spectrum of IECB. As compared to FTIR spectrum of chitosan, FTIR spectrum of IEC beads possess some shifts such as at wavenumber 1031 cm^{-1}, which confirms the linkage of chitosan in the solution. [122] First of all a band lies at 556 cm^{-1}, which is related to the rhombohedral oscillations of Fe-O functional grup. The peaks at 1364 cm^{-1} and at 1594 cm^{-1} are attributed to the vibrations of CH functional group and –NH group. 2869 cm^{-1} corresponds to the vibrational stretch of mathyl (-CH_3) and mathylene (-CH_2) functional groups (C-H) which originally belong to chitosan. [123] Moreover, the strong broad bands at the range of (3200 cm^{-1} -3400. cm^{-1}) shows the presence of NH_2 and OH in the magnetic chitosan beads. These results effectively concluded the presence of cross linked chitosan in the beads. [124]

4.3.3 FTIR of IECB after Cr (VI) adsorption

FTIR spectrum of Iron Oxide embedded chitosan beads has shown in the figure 19 (c). It has been observed, that two new bands have been appeared in the spectrum at wavenumber of 785cm^{-1} and 901cm^{-1} after Cr (VI) adsorption. These bands refer to the oscillations of Cr - O and Cr = O bonds, which shows adsorption of some Cr (VI) ions on beads. Moreover, after Cr (VI) adsorption proportion of O increases because of it. [125]

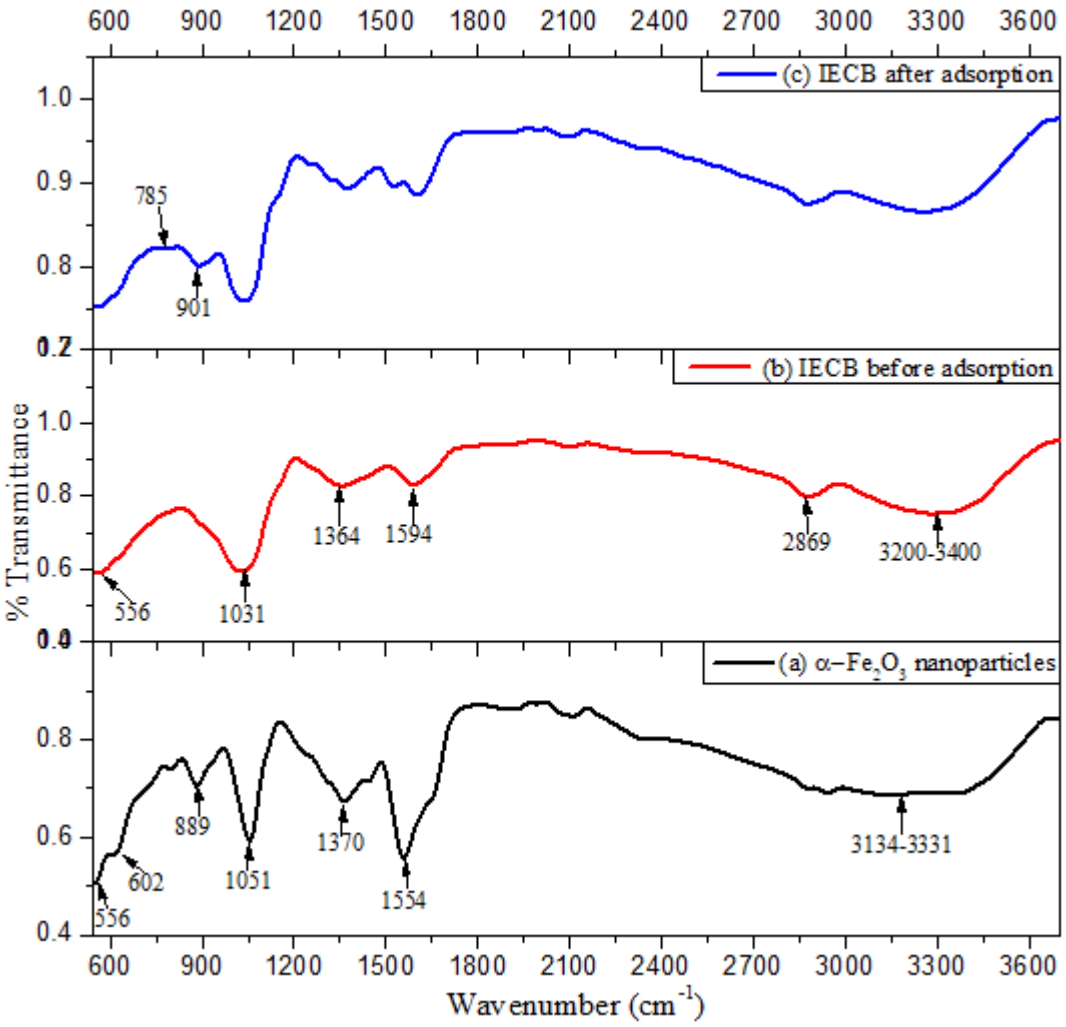

Figure 19: FTIR of (a) α-Fe_2O_3 nanoparticles (b) IECB before adsorption (c) IECB after adsorption

4.4 Vibrating-sample magnetometer

4.4.1 Vibrating-sample magnetometer analysis for Iron Oxide NPs

VSM study demonstrate the appearance and largeness reliance of hypnotic properties of Iron Oxide NPs that is coarcivity and saturation magnatization. Iron Oxide NPs is an important magnetic material, due to the morphology and size of the particles they possess special properties. Figure 20 (a) shows hysteresis magnetic loop taken at room temperature. Current study's results explains the weak ferromagnetic nature of the specimen. [103] in this study NPs has a Remanant magnatization value of 0.012 emu/g,

coersive magnetic field of 222 Oe and saturation magnetization of 0.443emu/g. This low coersivity is due to the small size of NPs. [104] as size of the NPs is not too small which can give surface spin interaction, so saturation magnetization is also small. Sometimes crystal defects and disorders in nanostructures also give small saturation magnetization. [105]

4.4.2 Vibrating-sample magnetometer analysis of Beads

As compared to iron oxide NPs, Iron Oxide embedded chitosan beads will show reduced values of Remanent magnetization, coersive magnetic field and specially saturation magnetization. Figure 20 (b) shows the lessen value of Remanent magnatization from 0.012 emu/g to 0.0059 emu/g, Coersivity from 222 Oe to 99.5 Oe and saturation magnetization (Ms) from 0.443 emu/g to 0.430 emu/g. [106] to assess the recuperation capability of Iron Oxide NPs embedded chitosan beads using a magnet after adsorption, the value of Ms Plays an important role. Lower value of Ms may be corresponds to the surface modification of NPs by CS. [107] as these polymers will induce an additional cross-link shielding of non-magnetic matrix, which will restrict the magnetic coupling interactions of magnetic NPs. Due to very minute reduction in Ms, magnetic beads will possess weak ferromagnetic nature and can be utilized as magnetic material for removal purpose of heavy metal ions. [108]

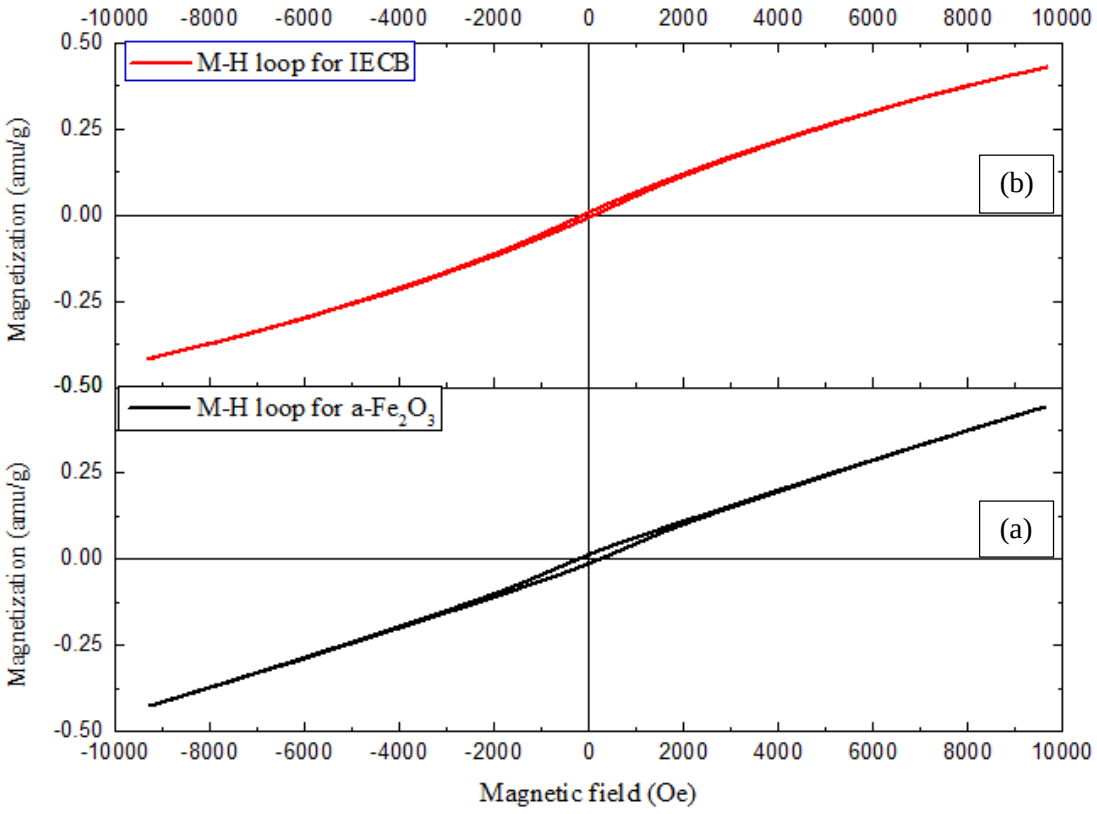

Figure 20: VSM measurements for (a) α-Fe_2O_3 (b) IECB

4.5 Contact angle measurement

Contact angle of iron oxide embedded chitosan beads (B1, B2, B3) has been shown in figure 21. According to the contact angle measurements of the beads, they posess hydrophyllic nature, which is due to the existence of NH_3 of pure chitosan on the outer surface of the beads. The contact angle of B3 with Deionized water has value i.e.58.97°. However, because of the presence of chitosan in less amount, other samples are little bit more hydrophilic comparitively. [99] As contact angle lower than 90° gives better wetting conditions upon the surface of the beads, which will increase the adhesiveness and surface energy of the beads, which will ultimately enhance the adsorption properties of the beads. [100]

Table 3: Contact Angles of magnetic beasds

Beads	Contact angle
Bead 1	51.76◦
Bead 2	54.24◦
Bead 3	58.97◦

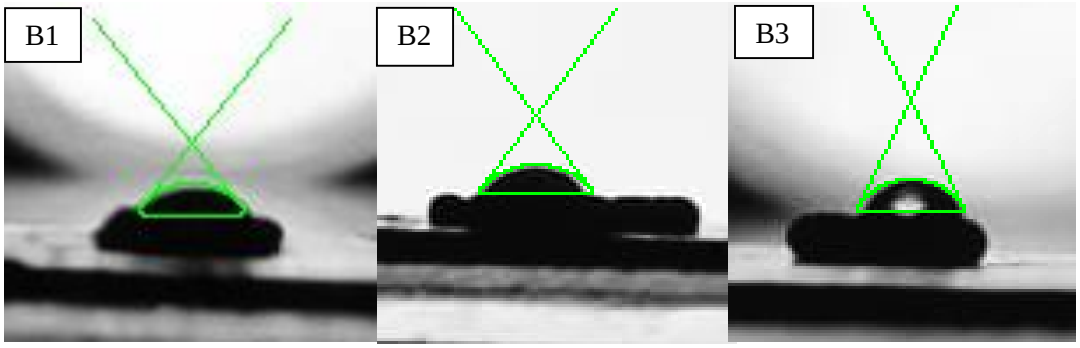

Figure 21 : Wetting behaviour of B1, B2, B3

4.6 Brunauer–Emmett–Teller (BET) analysis

According to the adsorption-desorption (BET) isotherms the quantity of adsorbed N_2 was continuously increasing with increasing P/P_o, Which indicates a distribution of small pore size in the iron oxide embedded chitosan beads as shown in figure 22. The BET analysis based on the BJH method along with the results of pore volume of adsorbent bead, its pore size and porosity percentage is shown in the table 4 respectively. Such structure of adsorbent beads may facilitate the fast diffusion of Chromium ions during the process of adsorption. [102]

Archimede's Rule can be used to measure the porosity of the Iron Oxide embedded chitosan beads. According to this method firstly we have to measure the wright of the dry sample, then measure the weight of the fully saturated sample (beads) with solvent (ethanol) and the density of solvent must be known i.e. $0.789 g/cm^3$. Then, measure the weight of the saturated sample and again submerged it in the solvent (ethanol). Finally,

porosity of the samples can be calculated with the help of following equations by using above data. [101]

$$\mathbf{P} = \frac{\mathbf{Vp}}{\mathbf{Vb}}$$

$$\mathbf{Vp} = \frac{\mathbf{Mw} - \mathbf{Md}}{\mathbf{Pf}}$$

$$\mathbf{Vb} = \frac{\mathbf{Mw} - \mathbf{Ms}}{\mathbf{Pf}}$$

$$\mathbf{P\%} = \frac{\mathbf{Mw} - \mathbf{Md}}{\mathbf{Mw} - \mathbf{Ms}} \times \mathbf{100}$$

Where,

Vp is the pore volume, Vb is the bulk volume

P is the pore of the product

P_f is the m/V of ethanol g/cm^3

Md is the mass of specimen (g)

Mw is the mass of specimen saturated with ethanol (g)

Ms is the weight of saturated sample submerged in ethanol (g)

Table 4: Pore Width, Pore Volume and Porosity percentage studies

Beads	Pore volume (cm^3/g)	Pore width (A^0)	Porosity (%)
B1	0.00196	73.23	65.2
B2	0.00159	72.81	61.5
B3	0.00089	65.88	58.6

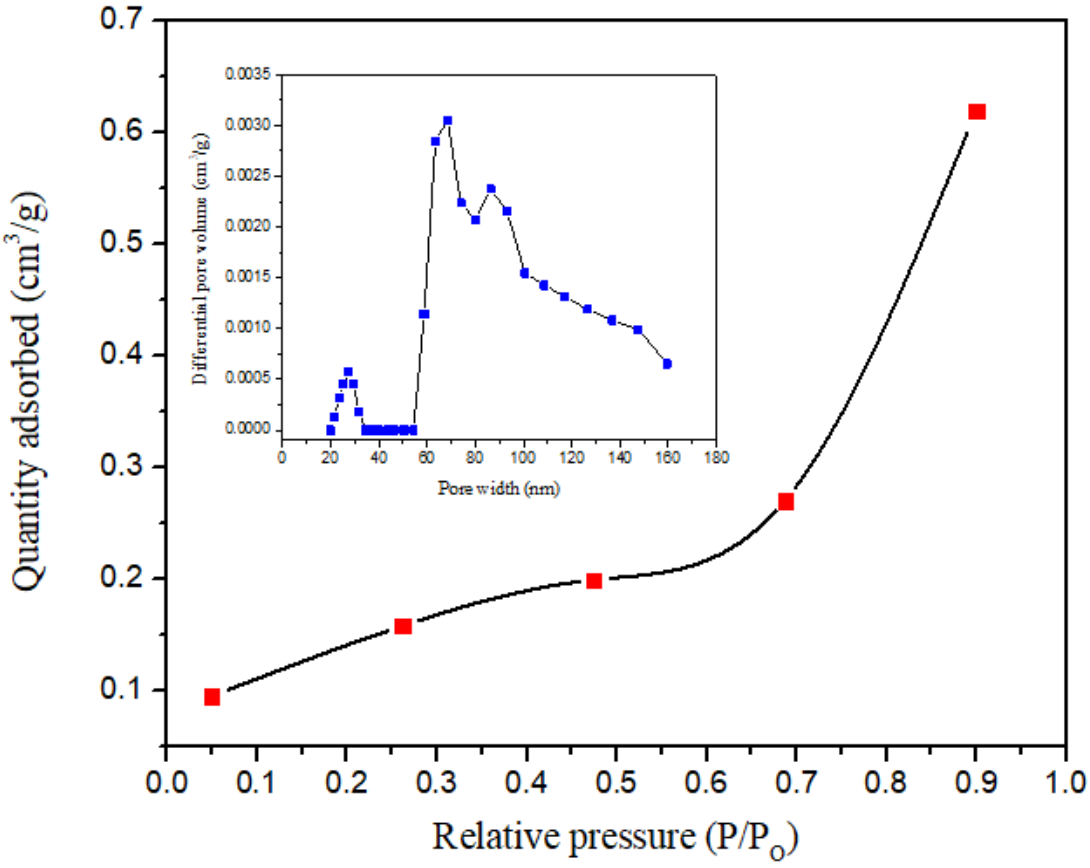

Figure 22: BET of IECB

4.7 Adsorption study

In adsorption experiment (400mg) beads were added into (1L) solution of Chromium. Constantly, stirring by a magnetic stirrer for six hours in order to remove the chromium and absorb onto the iron oxide embedded chitosan beads. Specimens were extracted from the flask at pre-arranged interval of time and concentration of Chromium analyzed through UV Vis spectroscopy. Finally, the capacity of Chromium adsorption by adsorbent was calculated by formula.

$$\boldsymbol{Qe = \frac{Co - Ce \times V}{m}}$$

Here, "Qe" is the beads's capacity of adsorption (mg/g), "C0" and "CE" is the starting and last (Cr) concentration (mg/l) accordingly. "V" is the velum of mixture (L), "m" is the weight of beads (g). By using UV Vis spectroscopy we can analyze the remaining amount of Chromium in aqeaous that is 0.414 (mg/l) which attributed that the 95% removal of Chromium is achieved in six hours. The removal efficiency can be calculated by using following formula.

$$\boldsymbol{Removal\ Efficiency}\ (\%) = \frac{(\boldsymbol{Initial\ con. - Final\ conc.})}{(\boldsymbol{Final\ conc.})} \times \mathbf{100}$$

4.7.1 Adsorption Isotherm

The concentration of the Cr substances on the bead from the solution could be evaluated with the aid of adsorptin isotherme i.e. Langmur and frendlich isotherm models at constant temperature.

4.7.1.1Langmuir Isotherm Model

Table 5: Regression value of Langmuir model

Langmuir Model		
Q_{max} (mg/g)	**K_L (L/mg)**	**R^2**
136.98	0.146	0.9917

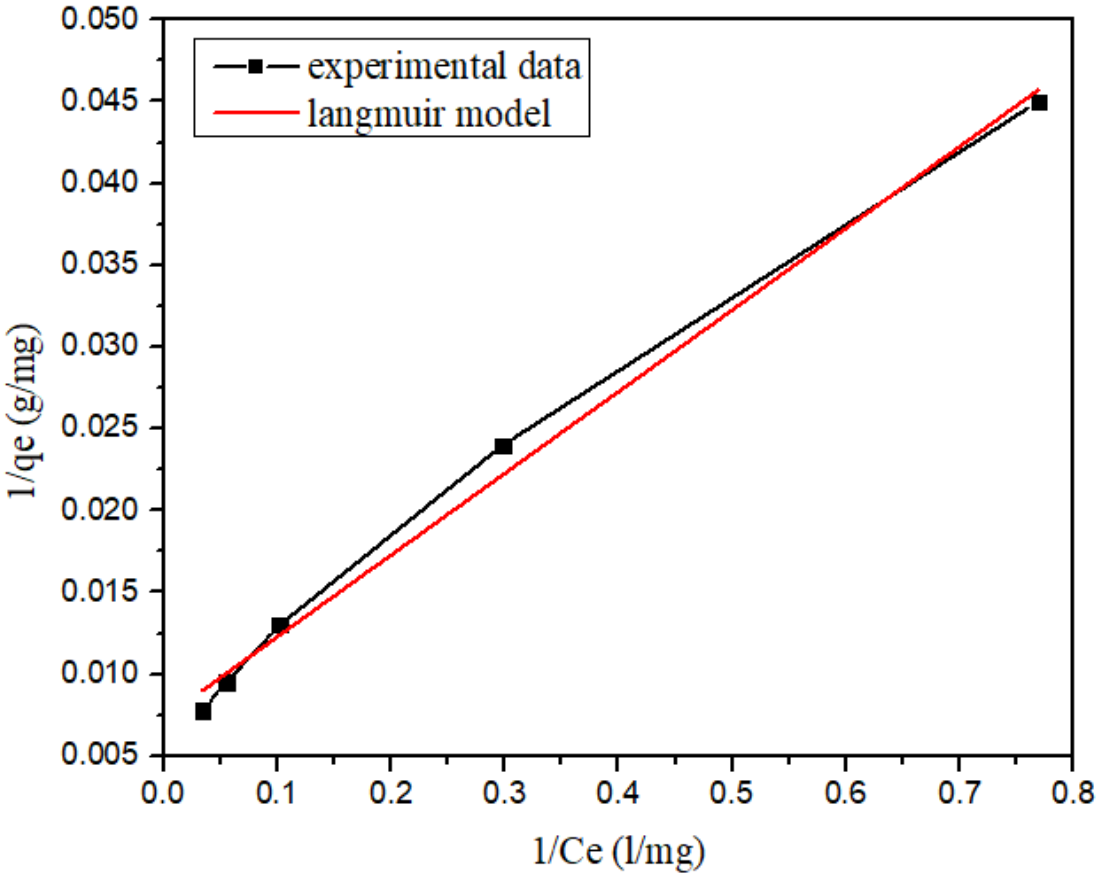

Figure 23: Graphical Representation of Langmuir Model

4.7.1.2Freundlich Isotherm Model

Table 6: Regression value of Freundlich isotherm model

Freundlich Model		
K	**N**	**R^2**
19.588	1.748	0.9905

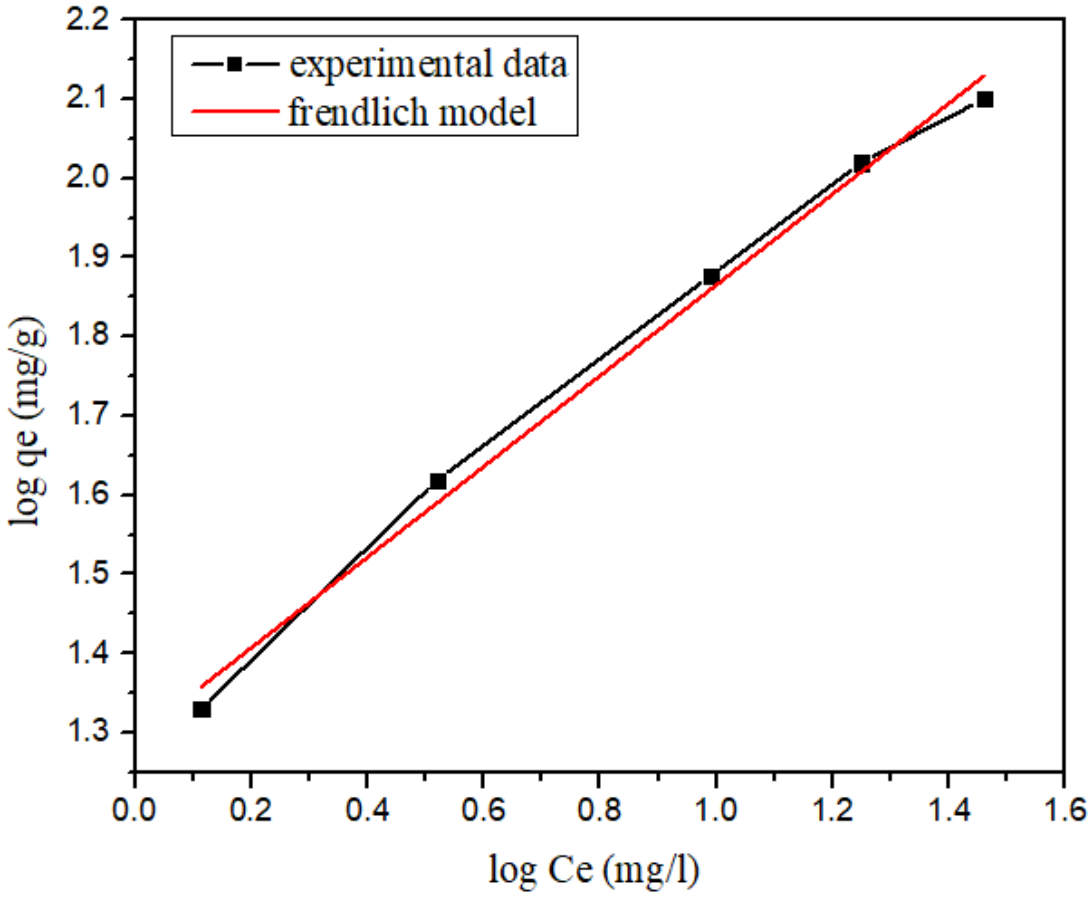

Figure 24: Graphical Representation of Freundlich Isotherm Model

4.7.2 Adsorption kinetics

The general assessment of the adsorption procedure is determined with the aid of adsorption knight i.e. pseuodo-first-order and pseuodo-second-order reactions. [33]

4.7.2.1Pseudo-First Order:

Table 7: Regression value of Psudo-First Order

Psudo First Order		
Qe (mg/g)	**K_1**	**R^2**
141.82	-5.38 x 10^-5	0.544

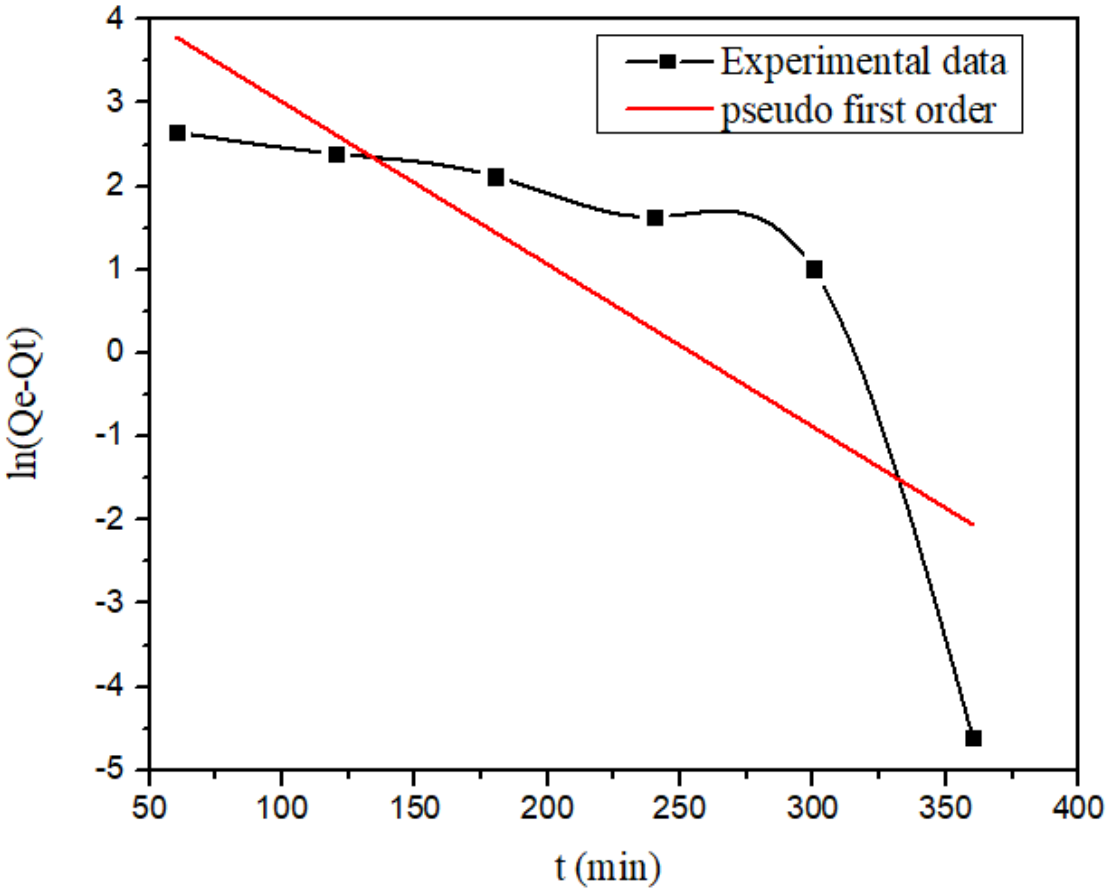

Figure 25: Graphical Representation of Pseudo-First Order data

Value of R^2 proved that, psudo Firsts order cannot give the perfection for the available preliminary data. Moreover, better relevance of the psudo firsts order appears to be associated with weak Cr (VI)-sorbent interaction i.e. physisorption.

4.7.2.2Pseudo-Second Order:

Table 8: Regression value of Psudo-Second Order

Psudo-Second Order		
Qe (mg/g)	**K_2 (h. g/mg)**	**R^2**
22.07	2.60 x 10^-4	0.984

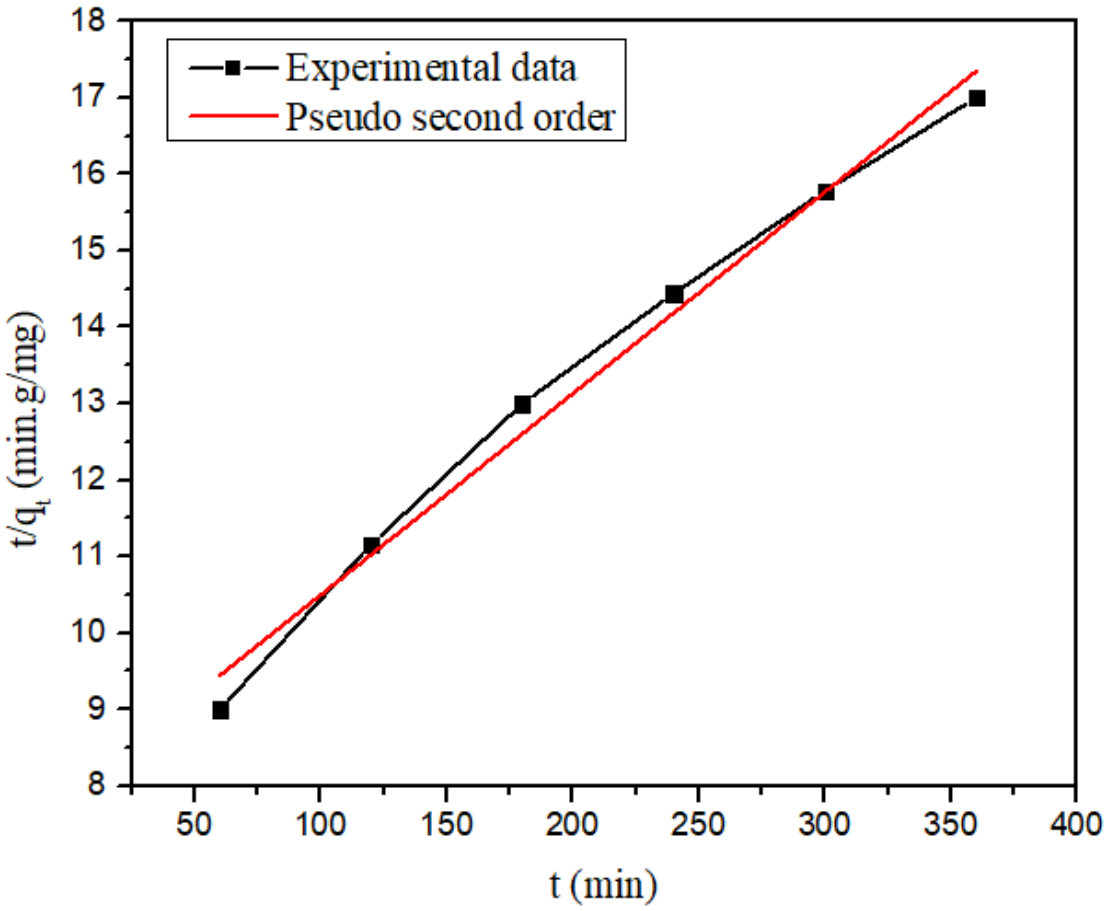

Figure 26: Graphical Representation of Pseudo-Second Order data

Depending on the value of R^2, pseudo second order can provide the perfection in the available preliminary measurements. According to the final outcomes, the current absorption methodology confirmed technically to the pseudo second order and the whole procedure should be dominated by chemisorption instead of physisorption. [88]

4.8 Influence of Different Parameters

1. pH
2. Time
3. Temperature
4. Starting concentration

4.8.1 Influence of Ph

pH of the solution has been considered as a crucial factor in order for the elimination of Cr from within waste water via adsorptin process. pH of the mixture greatly affect the exterior charge calculation of the adsorbant, the level of excitation and essentially it will have an immense impact on the speciation of adsorbate. In this examination, adsorptin of Cr (VI) was calculated at pH from (3-8) by using 40 mg beads and 100 ml chromium solution. [89] The Cr (VI) removal efficiency increases from pH (3-4) due to negatively charged adsorbent and adsorbate is positively charged, which leads to higher Cr uptake. [90] so maximum adsorption occur at pH 4 as shown in figure 27. Above pH 4 adsorptin of Cr (VI) starts decreasing. It is due to the presence of weak coordination bond between Cr (VI) ions and adsorbent functional groups. [91]

4.8.2 Influence of temperature

The adsorption of Cr was calculated for 4 varying temperatures (20, 40, 60 and 70 ◦C) by using 40 mg of iron oxide embedded chitosan beads with 100 mL of 10 mg/L Cr (VI) mixture toward pH 4 with 4 hours. The effect of varying heat upon the adsorptin of Cr (VI) by iron oxide embedded chitosan beads was given in Figure 27. [92] In this study Cr (VI) concentration in the mixture minimizes along with the high in heat. Whereas rise in temperature will increases the number of active positions accessible for reaction with Cr (VI) ions, which will enhance rate of adsorption ultimately. [93]

4.8.3 Influence of time

Contact time's impact on adsorption of Cr with the aid of iron oxide embedded chitosan beads was studied in 100ml of 10mg/L Cr (VI) mixture toward pH 4 along with bead's amount of 40mg at 24◦C. This assembly was stirred for six hours at 200rpm. Obtained results demonstrate that with the passage of time absorption of Cr (VI) ions was greatly enhanced as shown in figure 27. Most rapid adsorption occur over first six hours.

[94] Afterward adsorption will reach to an equilibrium level. This fashion might be due to complete filling of functional groups and drop in available adsorptions site. [95]

4.8.4 Influence of initial concentration

The impact of starting conc. of metal ions upon the adsorptin process was achieved at six varying metal concentrations (10, 40, 80 and 90mg/L) by using 40 mg of iron oxide embedded chitosan beads with 100 mL of Cr mixture at pH 4 for 6 hours. [96] as mentioned in the figure 27, at first the adsorptin magnitude of chitosan beds increased sharply along with higher initial concentration of metal ions. Main reason for it is that at high metal ions concentration, driving forces also increases via higher concentration gradients. [97] Even so, with the passage of time an equilibrium level of adsorption will be achieved because of drop in quantity of mobile adsorption sites. [98]

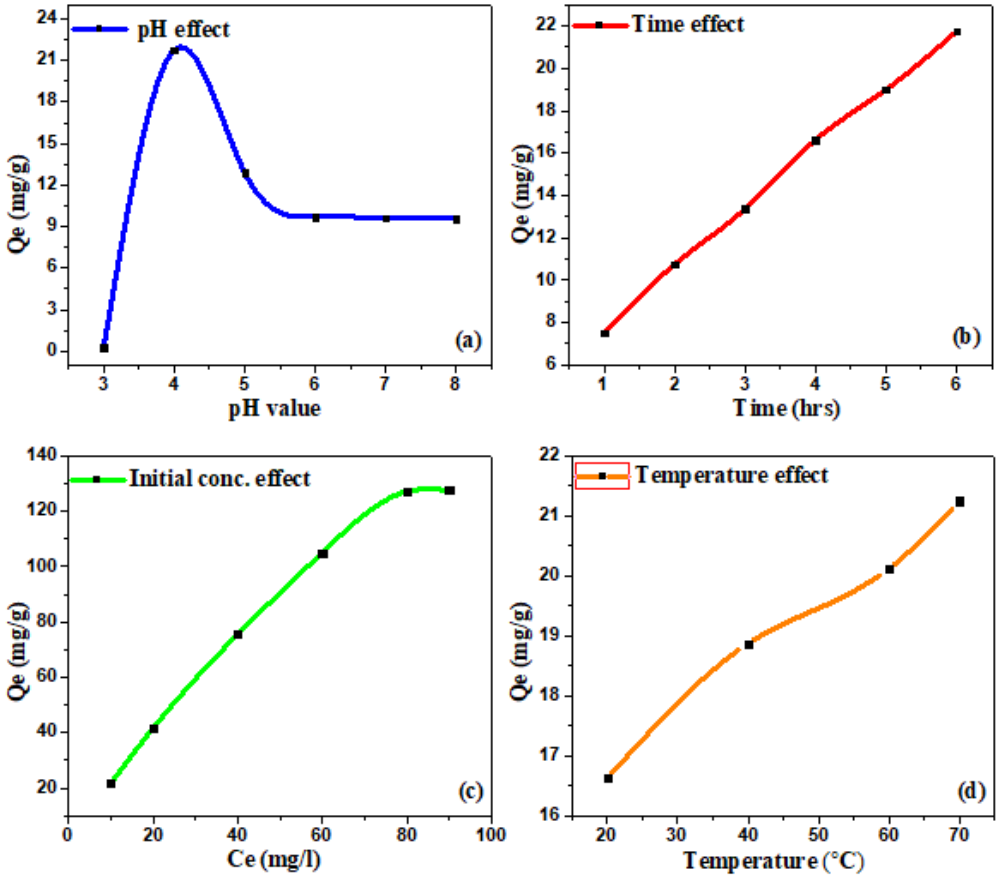

Figure 27: Graphical representation of influence of (a) pH (b) contact time (c) Initial conc. (d) Temperature on Cr(VI) adsorption

4.9 Regeneration Experiments

The regeneration of iron oxide embedded chitosan beads was carried out in a set of experiment. It was done by agitating the 200mg sample with in a beaker carrying 500ml of solution containing metal (10mg/L) with 70°C, 200rpm along with 4 pH during 6 h. Than the bead would washed properly to eliminate the unattached Cr (VI) rock metal ions. The Cr stuffed beads will be immersed within a 0.1 mol/L NaOH solution (250ml) and then shaked at 350 rpm with 25 °C toward 16 h then in final step wash with deionized water so that neutral pH obtained. After that, the IECB were arranged to dry at 60 °C for 6 h. Following performing the already mentioned steps, the IECB were reproduced as shown in figure 28. Recurrence of these adsorption/desorption cycles was done until significant decrease in the performance of beads occur.

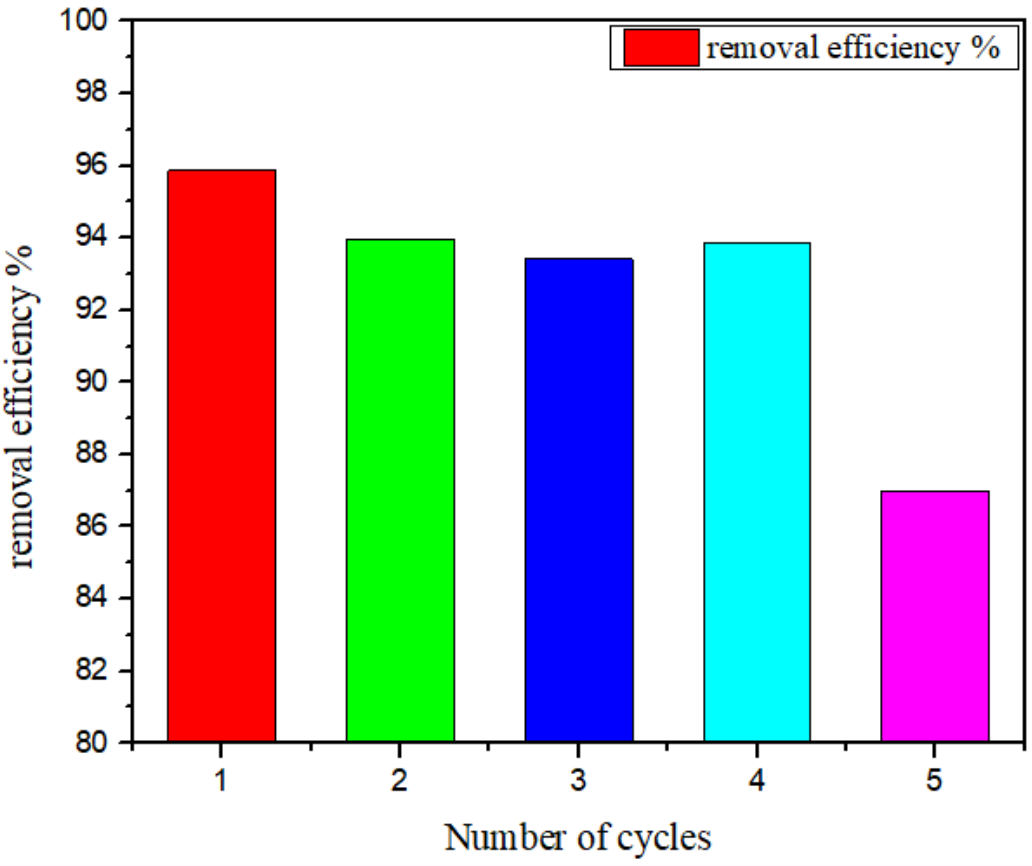

Figure 28: Regeneration of Iron Oxide embedded Chitosan beads

Conclusion

Nano scale Iron Oxide produced by Sol Gel process was embedded in chitosan by using chemical co-precipitation method and then prepared beads were used for the elimination of Cr (VI) from waste water. Characterization techniques like SEM and XRD demonstrated that rhombohedral shape α-Fe_2O_3 NPs lies in a complex form along with –OH and –NH_2 groups of chitosan in 1.6mm average size beads. Moreover, FTIR confirms the adhesion of Cr (VI) on sample beads by showing the presence of Cr-O and Cr=O bonds at 901cm^{-1} and 785cm^{-1}. Contact angle with value 58.9° and 58.6% porosity shows the hydrophilic nature of beads. Meanwhile, Current study shows greatly enhanced 23.9mg/g Cr (VI) adsorption capacity because of ligand exchange along with electrostatic attraction among Cr (VI) and amino groups lying on the bead's surface. Adsorption isotherm and kinetics study illustrate, that homogeneous single layer adsorption (Langmuir isotherm) was achieved with $R^2 > 0.991$ and chemisorption was the real rate controlling step (pseudo second order) with $R^2 > 0.984$. By utilizing 0.1 M NaOH, 87 % adsorption efficiency was successfully attained after 5 regeneration cycles. In nut shell, high adsorption capacity, easy magnetic separation, chemical stability, fast kinetics and renewability of IECB confirmed their great capability in water treatment.

Future Recommendations

Heavy metal contamination especially in drinking water could ultimately lead to death in serious cases. So for future recommendations, we can use these Iron Oxide embedded chitosan beads (IECB) for the elimination of other fatal heavy metal ions like Ni, As, Cd, Cu and Hg etc. which have been founded abundantly in the underground water as well as in industrial water. Moreover, efficiency of the beads can be enhanced tremendously by doing some modifications in them, like converting them into imprinted beads which will increase their productivity a lot in terms of selective adsorption of heavy metals.

References

[1] P. Rai, “Biomagnetic monitoring of particulate matter: in the Indo-Burma hotspot region”, Elsevier, (2015).

[2] M.W. Holdgate, “A Perspective of Environmental Pollution”. Cambridge Univ. Press, (1979).

[3] S. Singh, “Environmental Geography”, Prayag Pustak Bhawan, (1991), pp. 466–507.

[4] A.C. Stern, “Air Pollution: The effects of air pollution”, Elsevier, Vol. 2, (1977)

[5] L. West, “World water day: a billion people worldwide lack safe drinking water”, about. Com, (2006), pp.03-26.

[6] D. H. Pink, "Investing in Tomorrow's Liquid Gold", (2006)

[7] B. Moss, “Water pollution by agriculture”, Philosophical Transactions of the Royal Society B: Biological Sciences, Vol. 363, (2008), pp.659-666.

[8] A. E. Maczulak, “Pollution: Treating Environmental Toxins”, New York: Infobase Publishing, (2010), pp. 120.

[9] G. Banfalvi, “Cellular Effects of Heavy Metals”, Springer, (2011).

[10] N. Herawati, S. Suzuki, K. Hayashi, IF. Rivai, H. Koyoma, “Cadmium, copper and zinc levels in rice and soil of Japan, Indonesia and China by soil type”, Bulletin of Environmental Contamination and Toxicology, Vol. 64, (2000), pp. 33-39.

[11] W. Salomons, U. Forstner, P. Mader, “Heavy Metals: Problems and Solutions”, Berlin, Germany: Springer-Verlag, (1995).

[12] D. Brady, AD. Stoll, L. Starke, JR. Duncan, “Bioaccumulation of metal cations by Saccharomyces cerevisiae”, Applied Microbiology and Biotechnology, Vol. 41, (1994), pp. 149-154.

[13] WR. García-Niño, J. Pedraza-Chaverrí, “Protective effect of curcumin against heavy metals induced liver damage”, Food and Chemical Toxicology, Vol. 69, (2014), pp. 182-201.

[14] J. Emsley, (2011). “Nature’s Building Blocks: An A-Z Guide to the Elements”, Oxford, England, UK: Oxford University Press, (2011), pp. 495–498.

[15] J. Rieuwerts, “The Elements of Environmental Pollution” , London: Routledge, Vol. 1, (2015).

[16] T. Becquer, C. Quantin, M. Sicot, J. P. Boudot, “Chromium availability in ultramafic soils from New Caledonia”, The Science of the total environment, Vol. 301, (2003), pp. 251–261.

[17] J. R. Peralta-Videa, M. L. Lopez, M. Narayan, G. Saupe, J. Gardea-Torresdey, “The biochemistry of environmental heavy metal uptake by plants: implications for the food chain”, The international journal of biochemistry & cell biology, Vol. 41, (2009), pp. 1665–1677.

[18] K. Shekhawat, S. Chatterjee, B. Joshi, “Chromium toxicity and its health hazards”, International Journal of Advanced Research, Vol. 7, (2015), pp. 167-172.

[19] S. T. Matsumoto, M. S. Mantovani, M. I. A. Malaguttii, A. L. Dias, I. C. Fonseca, M. A. Marin-Morales, “Genotoxicity and mutagenicity of water contaminated with tannery effluents, as evaluated by the micronucleus test and comet assay using the fish Oreochromis niloticus and chromosome aberrations in onion root-tips”, Genetics Molecular Biology, Vol. 29, (2006), pp. 148-158.

[20] A. Zhitkovich, “Chromium in drinking water: sources, metabolism, and cancer risks”, Chemical research in toxicology, Vol. 24, (2011), pp. 1617–1629.

[21] C. E. Barrera-Díaz, V. Lugo-Lugo, B. Bilyeu, “A review of chemical, electrochemical and biological methods for aqueous Cr (VI) reduction”, Journal of hazardous materials, (2012), pp. 223-224.

[22] Y. Xing, X. Chen, D. Wang, “Electrically regenerated ion exchange for removal and recovery of Cr (VI) from wastewater”, Environmental science & technology, Vol. 41, (2007), pp. 1439–1443.

[23] A. Sawada, K. Mori, S. Tanaka, M. Fukushima, K. Tatsumi, “Removal of Cr (VI) from contaminated soil by electrokinetic remediation”, Waste management (New York), Vol. 24, (2004), pp. 483–490.

[24] V. K. Gupta, A. Nayak, S. Agarwal, “Bioadsorbents for remediation of heavy metals: Current status and their future prospects”, Environmental Engineering Research, Vol. 20, (2015), pp. 1–18.

[25] H. Deveci, Y. Kar, “Adsorption of hexavalent chromium from aqueous solutions by bio-chars obtained during biomass pyrolysis”, *J. Ind. Eng. Chem, Vol.* 19, (2013), pp. 190–196.

[26] J. Chen, X. Hong, Q. D. Xie, Q. F. Zhang, “Sepiolite fiber oriented-polypyrrole nanofibers for efficient chromium (VI) removal from aqueous solution”, Journal of Chemical & Engineering Data, Vol. 59, (2014), pp.2275–2282.

[27] R. Cossu, R. Stegmann, “Solid waste land filling: concepts, processes, technologies”, Amsterdam, Netherlands, Elsevier, (2019).

[28] T. Britannica, “Editors of Adsorption, Encyclopedia”, Britannica, (2013).

[29] L. Ferrari, J. Kaufmann, F. Winnefeld, J. Plank, "Interaction of cement model systems with superplasticizers investigated by atomic force microscopy, zeta potential, and adsorption measurements", J. Colloid Interface Sci, Vol. 347, (2010), pp. 15–24.

[30] E, Iakovleva, M. Sillanpää, “The Use of Low Cost Adsorbents for Wastewater Purification in Mining Industries”, Environmental Science and Pollution Research, Vol. 20, (2013), pp. 7878-7899.

[31] G. McKay, “Use of Adsorbents for the Removal of Pollutants from Wastewaters”, CRC Press, Inc. Hong Kong, (1996), pp. 40-43.

[32] E. Repo, “EDTA- and DTPA- Functionalized Silica Gel and Chitosan Adsorbents for the Removal of Heavy Metals From Aqueous Solutions”, Lappeenranta University of Technology, Thesis, (2011).

[33] T. Willis, “Sorbents – Properties, Materials and Applications”, Nova Science Publishers, Inc. New York, (2009), pp. 52-104.

[34] I. Langmuir, “The adsorption of gases on plane surface of glass, mica and platinum”, J Am Chem Soc, Vol. 40, (1916), pp. 1361–1403.

[35] H. M. F. Freundlich, “over the adsorption in solution”, J Phys Chem, Vol. 57, (1906), pp. 385–470.

[36] G. Crini, H.N. Peindy, F. Gimbert, C. Robert, (2007) “Separation and Purification Technology”, Vol. 53, (2007), pp. 97-110.

[37] E. Bulut, M. Ozacar, “Adsorption of malachite green onto bentonite: equilibrium and kinetic study and process design”, Micropor Mesopor Mat, Vol. 115, (2008), pp. 234–246.

[38] G. Tchobanoglous, F. L. Burton, Metcalf, Eddy, “Wastewater engineering: Treatment, disposal, and reuse”, New York, McGraw-Hill, (1991).

[39] Z. L. He, X. E. Yang, P.J. Stoffella, "Trace elements in agro ecosystems and impacts on the environment" Journal of trace elements in medicine and biology: organ of the Society for Minerals and Trace Elements (GMS), Vol. 19, (2005), pp. 125–140.

[40] Jha, K. Manis, Kumar, Vinay, L. Maharaj, R. J. Singh, "Studies on leaching and recycling of Zinc from rayon waste sludge", Industrial & Engineering Chemistry Research, Vol. 43, (2004), pp. 1284-1295.

[41] S. Kentish, G. Stevens, "Innovations in separations technology for the recycling and re-use of liquid waste streams", Chemical Engineering Journal, Vol. 84, (2001), pp. 149-159.

[42] M. K. Jha, R. R. Upadhyay, J. C. Lee, V. Kumar, "Treatment of rayon waste effluent for the removal of Zn and Ca using indion BSR resin", Desalination, Vol. 228, (2008), pp. 97–107.

[43] J. Xie, C. Xu, N. Kohler, Y. Hou, S. Sun, "Controlled PEGylation of monodisperse Fe3O4 nanoparticles for reduced non-specific uptake by macrophage cells", Adv. Mater, Vol. 19, (2007), pp. 3163–3166.

[44] S. Sun, H. Zeng, "Size-controlled synthesis of magnetite nanoparticles", Journal of the American Chemical Society, Vol. 124, (2002), pp. 8204–8205.

[45] S. Si, A. Kotal, T. K. Mandal, S. Giri, H. Nakamura, T. Kohara, "Size-controlled synthesis of magnetite nanoparticles in the presence of polyelectrolytes", Chem. Mater., Vol. 16, (2004), pp. 3489-3496.

[46] R. M. Cornell, U. Schwertmann, "The iron oxides: structure, properties, reactions, occurrences and uses", Wiley VCH, (2003).

[47] National Center for Biotechnology Information, "PubChem Compound Summary for CID 61560, Iron oxide (Fe2O3), hydrate", (2021).

[48] N. N. Greenwood, A. Earnshaw, "Chemistry of the Elements" (2nd Ed.). Butterworth-Heinemann, (1997).

[49] Pai, A. Barton, "Chapter 6. Iron Oxide Nanoparticle Formulations for Supplementation", Berlin: de Gruyter GmbH, (2019), pp. 157–180.

[50] A. K. Boal, "Synthesis and applications of magnetic nanoparticles, in: Nanoparticles", Springer, (2004), pp. 1-27.

[51] J. S. Walker, G. I. Straguzzi, W. H. Manogue, G. C. A. Schuit, “Carbon monoxide and propene oxidation by iron oxides for auto-emission control”, Journal of Catalysis, Vol. 110, (1988), pp. 298-309.

[52] P. Li, D. Miser, S. Rabiei, R. T. Yadav, “The removal of carbon monoxide by iron oxide nanoparticles”, Applied Catalysis B, Vol. 43, (2003), pp. 151-162.

[53] M. Tadić, N. Čitaković, M. Panjan, Z. Stojanović, D. Marković, V. Spasojević, “Synthesis, morphology, microstructure and magnetic properties of hematite submicron particles”, Journal of Alloys and Compounds, Vol. 509, (2011), pp. 7639–7644.

[54] M. M. Oliveira, D. C. Schnitzler, A. Zarbin, "(Ti,Sn)O_2 Mixed Oxides Nanoparticles Obtained by the Sol−Gel Route", Chemistry of Materials, Vol. 15, (2013), pp. 1903–1909.

[55] Xie, R. Cai, Shang, J. Ku, "Morphological control in solvothermal synthesis of titanium oxide", Journal of Materials Science, Vol. 42, (2007), pp. 6583–6589.

[56] S. Baykara, "Hydrogen production by direct solar thermal decomposition of water, possibilities for improvement of process efficiency", International Journal of Hydrogen Energy, Vol. 29, (2004), pp. 1451–1458.

[57] S. Belaïd, D. Stanicki, E. L. Vander, R. N. Muller, S. Laurent, “Influence of experimental parameters on iron oxide nanoparticle properties synthesized by thermal decomposition: size and nuclear magnetic resonance studies”, Nanotechnology, Vol. 29, (2018), pp. 165603.

[58] N. A. Frey, S. Peng, K. Cheng, S. Sun, “Magnetic nanoparticles: synthesis, functionalization, and applications in bioimaging and magnetic energy storage”, Chemical Society reviews, Vol. 38, (2009), pp. 2532–2542.

[59] W. Glasgow, B. Fellows, B. Qi, T. Darroudi, C. Kitchens, L. Ye, T. M. Crawford, O. T. Mefford, “Continuous synthesis of iron oxide (Fe3O4) nanoparticles via thermal decomposition”, Particuology, Vol. 26, (2016), pp. 47-53.

[60] F. B. Effenberger, R. A. Couto, P. K. Kiyohara, G. Machado, S. H. Masunaga, R. F. Jardim, L. M. Rossi, “Economically attractive route for the preparation of high quality magnetic nanoparticles by the thermal decomposition of iron(III) acetylacetonate”, Nanotechnology, Vol. 28, (2017), pp. 115603.

[61] Y. Gan, A. Jayatissa, Z. Yu, X. Chen, M. Li, “Hydrothermal Synthesis of Nanomaterials”, Journal of Nanomaterials, (2020), pp. 1-3.

[62] A.-H. Lu, E. L. Salabas, F. Schüth, "Magnetic Nanoparticles: Synthesis, Protection, Functionalization, and Application". Angew. Chem. Int. Ed. Vol. 46, (2007), pp. 1222–1244.

[63] J. H. Park, S. H. Shin, S. H. Kim, J. K. Park, J. W. Lee, J. H. Shin, J. H. Park, S. W. Kim, H. J. Choi, K. S. Lee, J. C. Ro, C. Park, S. J. Suh, “Effect of Synthesis Time and Composition on Magnetic Properties of FeCo Nanoparticles by Polyol Method”, Journal of nanoscience and nanotechnology, Vol. 18, (2018), pp. 7115–7119.

[64] G. Hemery, A. C. Keyes, Jr, E. Garaio, I. Rodrigo, J. A. Garcia, F. Plazaola, E. Garanger, O. Sandre, “Tuning Sizes, Morphologies, and Magnetic Properties of Monocore versus Multicore Iron Oxide Nanoparticles through the Controlled Addition of Water in the Polyol Synthesis” Inorganic chemistry, Vol. 56, (2017), pp. 8232–8243.

[65] S. Gupta, M. ripathi, “A review on the synthesis of TiO2 nanoparticles by solution route”, Central European Journal of Chemistry, Vol. 10 (2012).

[66] B. E. Yoldas, “Monolithic glass formation by chemical polymerization”, Journal of Materials Science, Vol. 14, (1979), pp. 1843-1849.

[67] G. W. Scherer, “Aging and drying of gels”, Journal of non-crystalline solids, Vol. 100, (1988), pp. 77-92.

[68] S. L. Isley, R. L. Penn, “Titanium Dioxide Nanoparticles: Effect of Sol−Gel pH on Phase Composition, Particle Size, and Particle Growth Mechanism”, The journal of physical chemistry C, Vol. 112, (2016), pp. 4469–4474.

[69] C. De Coelho Escobar, J. D. dos Santos, “Effect of the sol-gel route on the textural characteristics of silica imprinted with Rhodamine B”, Journal of separation science, Vol. 37(2014), pp. 868–875.

[70] L. L. Hench, J. K. West, “the Sol-Gel Process”, Chemical Reviews, Vol. 90, (1990), pp. 33-72.

[71] M. Niederberger, N. Pinna, “Metal oxide nanoparticles in organic solvents: synthesis, formation, assembly and application”, Springer, New York, (2009).

[72] M. M. Collinson, H. Wang, R. Makote, A. Khramov, (2002) “The Effects of Drying Time and Relative Humidity on the Stability of Sol-Gel Derived Silicate Films in Solution”, J. Electroanal. Chem, Vol. 519, (2002), pp. 65–71.

[73] G. Li, Z. Zhao, J. Liu, G. Jiang, “Effective heavy metal removal from aqueous systems by thiol functionalized magnetic mesoporous silica”, Journal of hazardous materials, Vol. 192, (2011), pp. 277–283.

[74] A. Z. Md. Badruddoza, Z. B. Z. Shawon, Md. T. Rahman, K. W. Hao, K. Hidajat, M. S. Uddin, “Ionically modified magnetic nanomaterials for arsenic and chromium removal from water”, Chemical Engineering Journal, Vol. 225, (2013), pp. 607–615.

[75] L. Qin, D. Yao, L. Zheng, W. C. Liu, Z. Liu, M. Lei, L. Huang, X. Xie, X. Wang, Y. Chen, X. Yao, J. Peng, H. Gong, J. F. Griffith, Y. Huang, Y. Zheng, J. Q. Feng, Y. Liu, S. Chen, D. Xiao, C. Y. Cheng, “Phytomolecule icaritin incorporated PLGA/TCP scaffold for steroid-associated osteonecrosis: Proof-of-concept for prevention of hip joint collapse in bipedal emus and mechanistic study in quadrupedal rabbits”, Biomaterials, Vol. 59, (2015), pp. 125–143.

[76] M. S. Chiou, P. Y. Ho, H. Y. Li, “Adsorption of Anionic Dyes in Acid Solutions Using Chemically Cross-Linked Chitosan Beads”, Dyes and Pigments, Vol. 60,(2004), pp. 69-84.

[77] N. Sakkayawong, P. Thiravetyan, W. Nakbanpote, “Adsorption mechanism of synthetic reactive dye wastewater by chitosan”, Journal of colloid and interface science, Vol. 286, (2005), pp. 36–42.

[78] V. M. Boddu, K. Abburi, J. L. Talbott, E. D. Smith, “Removal of hexavalent chromium from wastewater using a new composite chitosan biosorbent”, Environmental science & technology, Vol. 37, (2013), pp. 4449–4456.

[79] A. R. Kaveeshwar, M. Sanders, S. K. Ponnusamy, D. Depan, R. Subramaniam, “Chitosan as a biosorbent for adsorption of iron (II) from fracking wastewater”, Polym Adv Technol, Vol. 29, (2018), pp. 961–969.

[80] S. K. Gill, G. Singh, M. Khatri, “Synthesis and characterization of superparamagnetic iron oxide nanoparticles for water purification applications”, Int J Eng Technol Sci Res, Vol. 4, (2017), pp. 355–359.

[81] S. Zhang, L. Li, A. Kumar, “Materials characterization techniques”, Boca Raton: CRC Press, (2009).

[82] Stokes, J. Debbie, “Principles and Practice of Variable Pressure Environmental Scanning Electron Microscopy (VP-ESEM)”, Chichester: John Wiley & Sons, (2008).

[83] D. A. Skoog, F. J. Holler, S. R. Crouch, “Principles of Instrumental Analysis Belmont, CA: Thomson Brooks/Cole, (2007), pp. 169–173.

[84] P. Griffiths, J. A. de Hasseth, “Fourier Transform Infrared Spectrometry”, Wiley-Blackwell, (2007).

[85] "The Infracord double-beam spectrophotometer", Clinical Science, Vol. 16, (1957).

[86] A. W. Coats, J. P. Redfern, "Thermogravimetric Analysis: A Review". Analyst, Vol. 88, (1963), pp. 906–924.

[87] J. R. Connolly, “Introduction to X-Ray Powder Diffraction”, (2007).

[88] M. Yurdakoç, Y. Seki, S. Karahan, K. Yurdakoç, “Kinetic and thermodynamic studies of boron removal by Siral 5, Siral 40, and Siral 80”, Journal of colloid and interface science, Vol. 286, (2005), pp. 440–446.

[89] R. Schmuhl, H. M. Krieg, K. Keizer, “Adsorption of Cu (II) and Cr (VI) Ions by Chitosan: Kinetics and Equilibrium Studies”, Water SA, Vol. 27, (2001), pp. 1–7.

[90] S. Babel, T. A. Kurniawan, “Cr (VI) removal from synthetic wastewater using coconut shell charcoal and commercial activated carbon modified with oxidizing agents and/or chitosan”, Chemosphere, Vol. 54, (2004), pp. 951–967.

[91] G. Huang, H. Zhang, J. X. Shi, T. A. G. Langrish, “Adsorption of Chromium (VI) from Aqueous Solutions Using Cross-Linked Magnetic Chitosan Beads”, Industrial & Engineering Chemistry Research, Vol, 48, (2009), pp. 2646–2651.

[92] Y. G. Abou El-Reash, M. Otto, I. M. Kenawy, A. M. Ouf, “Adsorption of Cr (VI) and As (V) ions by modified magnetic chitosan chelating resin”, International journal of biological macromolecules, Vol. 49, (2011), pp. 513–522.

[93] A. Hamouda, S. Ahmed, N. Mohamed, M. Khalil, “Adsorption of Cr (VI) from Aqueous Solution by Glycine Modified Cross-linked Chitosan Resin”, Egyptian Journal of Chemistry, Vol. 61, (2018), pp. 799-812.

[94] M. Vakili, S. Deng, D. Liu, T. Li, G. Yu, “Preparation of aminated cross-linked chitosan beads for efficient adsorption of hexavalent chromium”, International journal of biological macromolecules, Vol. 139, (2019), pp. 352–360.

[95] M. Vakili, M. Rafatullah, M. H. Ibrahim, A. Z. Abdullah, B. Salamatinia, Z. Gholami, “Chitosan hydrogel beads impregnated with hexadecylamine for improved reactive blue 4 adsorption”, Carbohydrate polymers, Vol. 137, (2016), pp. 139–146.

[96] B. H. Hameed, A. A. Ahmad, N. Aziz, “Isotherms, kinetics and thermodynamics of acid dye adsorption on activated palm ash”, Chemical Engineering Journal, Vol. 133, (2007), pp. 195–203.

[97] Y. G. Abou El-Reash, “Magnetic chitosan modified with cysteine-glutaraldehyde as adsorbent for removal of heavy metals from water”, Journal of Environmental Chemical Engineering, Vol. 4, (2016), pp. 3835–3847.

[98] M. Monier, D. M. Ayad, Y. Wei, A. A. Sarhan, “Adsorption of Cu (II), Co (II), and Ni (II) ions by modified magnetic chitosan chelating resin”, Journal of Hazardous Materials, Vol. 177, (2010), pp. 962–970.

[99] S. S. Shenvi, S. A. Rashid, A. F. Ismail, M. A. Kassim, A. M. Isloor, “Preparation and characterization of PPEES/chitosan composite nanofiltration membrane”, Desalination, Vol. 315, (2013), pp. 135–141.

[100] H. Y. Lin, C. T. Yeh, “Controlled release of pentoxifylline from porous chitosan-pectin scaffolds”, Drug Delivery, Vol. 17, (2010), pp. 313–321.

[101] T. De Terris, O. Andreau, P. Peyre, F. Adamski, I. Koutiri, C. Gorny, C. Dupuy, “Optimization and comparison of porosity rate measurement methods of Selective Laser Melted metallic parts”, Additive Manufacturing, (2019).

[102] B. Bai, X. Xu, C. Li, J. Xing, H. Wang, Y. Suo, “Magnetic Fe3O4@Chitosan Carbon Microbeads: Removal of Doxycycline from Aqueous Solutions through a Fixed Bed via Sequential Adsorption and Heterogeneous Fenton-Like Regeneration”, Journal of Nanomaterials, (2018), pp. 1–14.

[103] H. Ni, Y. Ni, Y. Zhou, J. Hong, “Microwave–hydrothermal synthesis, characterization and properties of rice-like α-Fe2O3 nanorods”, Materials Letters, Vol. 73, (2012), pp. 206–208.

[104] M. Sirena, A. Zimmers, N. Haberkorn, E. Kaul, L. B. Steren, J. Lesueur, G. Faini, “Direct observation of electronic inhomogeneities induced by point defect disorder in manganite films”, Journal of Applied Physics, Vol. 107, (2010), pp. 113903.

[105] Z. Cheng, A. L. K. Tan, Y. Tao, D. Shan, K. E. Ting, X. Y. Yin, “Synthesis and Characterization of Iron Oxide Nanoparticles and Applications in the Removal of Heavy Metals from Industrial Wastewater” International Journal of Photoenergy, (2012), pp. 1–5.

[106] H. Mo, J. Qiu, “Preparation of Chitosan/Magnetic Porous Biochar as Support for Cellulase Immobilization by Using Glutaraldehyde”, Polymers, Vol. 12, (2020), pp. 2672.

[107] M. P. Kesavan, S. Ayyanaar, V. Vijayakumar, R. J. Dhaveethu, J. Annaraj, K. Sakthipandi, J. Rajesh, “Magnetic iron oxide nanoparticles (MIONs) cross-linked natural polymer-based hybrid gel beads: Controlled nano anti-TB drug delivery application”, Journal of biomedical materials research. Part A, Vol. 106, (2018), pp. 1039–1050.

[108] S. Liu, B. Huang, L. Chai, Y. Liu, G. Zeng, X. Wang, Z. Zhou, “Enhancement of As (v) adsorption from aqueous solution by a magnetic chitosan/biochar composite”, RSC Advances, Vol. 7, (2017), pp. 10891–10900.

[109] C. Wang, J. Shi, X. Cui, H. Wang, J. Wu, C. Zhang, Y. Xu, “Nonspherical hollow α-Fe2O3 structures synthesized by stepwise effect of fluoride and phosphate anions”, Journal of Materials Chemistry A, Vol. 4, (2016), pp. 11000–11008.

[110] A. N. S. Rufus, D. Philip, “Synthesis of biogenic hematite (α-Fe2O3) nanoparticles for antibacterial and nanofluid applications”, RSC Advances, Vol. 6, (2016), pp. 94206–94217.

[111] L. Zhang, W. Xia, B. Teng, X. Liu, W. Zhang, “Zirconium cross-linked chitosan composite: Preparation, characterization and application in adsorption of Cr (VI)”, Chemical Engineering Journal, Vol. 229, (2013), pp. 1-8.

[112] Chagas P. M. B, Carvalho L. B. de, Caetano A. A, Nogueira F. G. E, Corrêa A. D, Guimarães I. d. R, “Nanostructured oxide stabilized by chitosan: hybrid composite as an adsorbent for the removal of chromium (VI)”, J Environ Chem Eng, Vol. 6, (2018), pp. 1008–1019.

[113] Chagas P. M. B, Caetano A. A, Rossi M. A, Gonçalves M. A, de Castro Ramalho T, Corrêa A. D, do Rosário Guimarães I, "Chitosan-iron oxide hybrid composite: mechanism of hexavalent chromium removal by central composite design and theoretical calculations", Environmental Science and Pollution Research, (2019).

[114] A. Rajeswari, A. Amalraj, A. Pius, "Adsorption studies for the removal of nitrate using chitosan/PEG and chitosan/PVA polymer composites", Journal of Water Process Engineering, Vol. 9, (2016), pp. 123–134.

[115] Y. Zhao, L. Guo, W. Shen, Q. An, Z. Xiao, H. Wang, Z. Li, "Function integrated chitosan-based beads with throughout sorption sites and inherent diffusion network for efficient phosphate removal", Carbohydrate Polymers, (2019), pp. 115639.

[116] M. M. Ba-Abbad, M. S. Takriff, A. Benamor, A. W. Mohammad, "Size and shape controlled of α-Fe2O3 nanoparticles prepared via sol–gel technique and their photocatalytic activity", Journal of Sol-Gel Science and Technology, Vol. 81, (2016), pp. 880–893.

[117] D. Malwal, P. Gopinath, "Silica Stabilized Magnetic-Chitosan Beads for Removal of Arsenic from Water", Colloid and Interface Science Communications, Vol. 19, (2017), pp. 14–19.

[118] M. I. Shariful, T. Sepehr, M. Mehrali, B. C. Ang, M. A. Amalina, "Adsorption capability of heavy metals by chitosan/poly (ethylene oxide)/activated carbon electrospun nanofibrous membrane", Journal of Applied Polymer Science, Vol. 135, (2017), pp. 45851.

[119] W. Qin, C. Yang, R. Yi, G. Gao, "Hydrothermal Synthesis and Characterization of Single-Crystalline -Fe2O3Nanocubes", Journal of Nanomaterials, (2011), pp. 1–5.

[120] A. Lassoued, B. Dkhil, A. Gadri, S. Ammar, "Control of the shape and size of iron oxide (α-Fe_2O_3) nanoparticles synthesized through the chemical precipitation method", Results in Physics, Vol. 7, (2017), pp. 3007–3015.

[121] Y. Chen, J. Wang, "Removal of radionuclide Sr2+ ions from aqueous solution using synthesized magnetic chitosan beads", Nuclear Engineering and Design, Vol. 242, (2012), pp. 445–451.

[122] Rahmi, Fathurrahmi, Lelifajri, F. Purnamawati, R. Sembiring, “Preparation of Magnetic Chitosan Beads for Heavy Metal Ions Removal from Water”, IOP Conference Series: Earth and Environmental Science, Vol. 276, (2019), pp. 012004.

[123] R. B. Hernández, A. P. Franco, O. R. Yola, A. López-Delgado, J. Felcman, M. A. L. Recio, A. L. R, “Coordination study of chitosan and Fe3+”, Journal of Molecular Structure, Vol. 877, (2008), pp. 89-99.

[124] K. Z. Elwakeel, E. Guibal, “Arsenic (V) sorption using chitosan/Cu (OH) 2 and chitosan/CuO composite sorbents”, Carbohydrate Polymers, Vol. 134, (2015), pp. 190–204.

[125] S. DENG, “Removal of trivalent and hexavalent chromium with aminated polyacrylonitrile fibers: performance and mechanisms”, Water Research, Vol. 38, (2004), pp. 2424–2432.